

# Consistent meson-field-theoretical description of $pp$ bremsstrahlung

J. A. Eden\* and M. F. Gari

*Institut für Theoretische Physik, Ruhr Universität Bochum, D-44780 Bochum, Germany*

(Received 31 March 1995)

A parameter-free and relativistic extension of the RuhrPot meson-baryon model is used to define the dominant isoscalar meson-exchange currents. We compute  $pp$ -bremsstrahlung observables below the  $\pi$ -production threshold using a relativistic hadronic current density that includes impulse, wave function reorthonormalization, meson-recoil,  $\bar{N}N$  creation and annihilation,  $\rho\pi\gamma + \omega\pi\gamma + \rho\eta\gamma + \omega\eta\gamma$  vector-meson decay, and  $N\Delta\gamma(\pi,\rho)$  exchange currents. We obtain a good description of the available data. The  $N\Delta\gamma(\pi)$  current is shown to dominate the large two-body contributions and closed-form expressions for various non-relativistic approximations are analyzed. An experimental sensitivity to the admixture of pseudoscalar and pseudovector admixture of the  $NN\pi$  interaction is demonstrated. We examine the Lorentz invariance of the  $NN\Rightarrow NN$   $t$  matrices and show a dominantly pseudovector  $NN\pi$  coupling renders impulse approximation calculations without boost operators to be essentially exact. Conversely, a similar analysis of the  $\Delta N\Rightarrow NN$  transitions shows that boost operators and the two-body  $N\Delta\gamma$  wave function reorthonormalization meson-recoil currents are required in  $NN$ ,  $\Delta N$ , and  $\Delta\Delta$  coupled channel  $t$ -matrix applications. The need for additional data is stressed.

PACS number(s): 13.75.Cs, 25.20.Lj

## I. INTRODUCTION

The realization that meson-exchange currents play a vital role in the description of the low-energy  $pp$ -bremsstrahlung observables has consequences which are only now coming to be understood. For example, the traditional objective of  $pp$ -bremsstrahlung investigations, as indicated in Fig. 1, centers on the capacity of experiment to differentiate the accuracy of the off-shell  $t$  matrices that are predicted by a range of model-dependent  $NN$  interactions. This is now recognized [1,2] as an exceedingly difficult task and, at best, is contingent on a completely reliable and consistent description of the associated meson-exchange currents. As such, a meaningful calculation of the  $pp$ -bremsstrahlung observables requires knowledge of the meson-baryon form factors, meson-exchange currents, and the  $NN$  interaction within a fully consistent and microscopic effective theory.

Recognizing the importance of exchange currents in  $pp$ -bremsstrahlung implies a complete departure from the conventional approach to the problem and considerably changes the nature of such investigation. For many years  $pp$ -bremsstrahlung was regarded as something of a special case in nuclear physics because both meson-exchange currents and relativistic effects were expected to be small. The principle reason for this expectation stems from the fact that gauge invariance demands the real photon couples only to conserved currents, so that the  $n$ -body parts of the complete hadronic current  $J_{[n]}$  for any given  $NN$  interaction  $V_{NN}$  must satisfy

$$0 = \nabla \cdot \vec{J} + i[\mathcal{H}, J^0],$$

$$\Rightarrow 0 = \begin{cases} \nabla \cdot \vec{J}_{[1]} + i[H_0, J_{[1]}^0] & \text{(one body),} \\ \nabla \cdot \vec{J}_{[2]} + i[V_{NN}, J_{[1]}^0] \\ \quad + i[H_0 + V_{NN}, J_{[2]}^0] & \text{(two body)} \end{cases} \quad (1.1)$$

To isolate the dominant contributions to the observables, it is useful to consider only the static limit, where the two-body charge density  $J_{[2]}^0$  can be ignored. The isospin structure of the exchange currents  $\vec{J}_{[2]}$  for isovector mesons ( $\pi, \rho, \dots$ ) then reduces to  $(\vec{\tau}_1 \times \vec{\tau}_2)^z$ , which vanishes in isospin conserving processes like  $pp$ -bremsstrahlung. Relativistic processes can also be expected to be small since the dominant  $\pi$ -exchange contributions to the  $\bar{N}\bar{N}$ -pair creation and annihilation amplitudes share this isospin structure. Finally, all  $NN\gamma$  couplings with meson-recoil terms can be neglected since they are exactly canceled by the corresponding wave function reorthonormalization contributions [3]. All of this information suggests that a static limit description of  $pp$ -bremsstrahlung involves only the photon coupling to one of the protons either before and/or after (but not during) strong interaction. The leading-order exchange currents, according to this analysis, begin with the  $\eta$  (549 MeV),  $\omega$  (782 MeV), and  $\epsilon$  (975 MeV) isoscalar mesons, and can therefore be reasonably neglected.

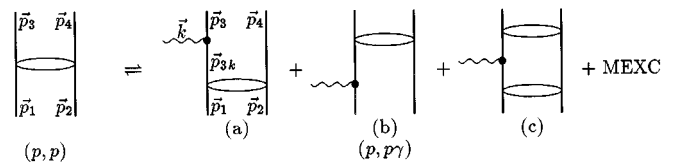


FIG. 1. Relationship between the on-shell  $t$  matrix in  $pp$  scattering,  $(p,p)$  and the off-shell  $t$  matrix in  $pp$  bremsstrahlung  $(p,p\gamma)$ . The parameters in the  $NN$  interaction  $V$  defining  $t = V + VGt$  (shown as a bubble) are fitted to the  $(N,N)$  phase shifts. Bremsstrahlung is usually considered in nucleon-pole dominance, where (a) initial, (b) final, and (c) rescattering interactions are retained, but all meson-exchange currents are neglected. Within this assumption, bremsstrahlung has been regarded as the best means of testing the off-shell  $t$  matrix. However, a sensitivity to off-shell effects requires a large photon energy, so that  $G = (E - H_0)^{-1}$  diminishes the dominant nucleon pole contributions and the exchange currents become important.

\*Electronic address: jamie@deuteron.tp2.ruhr-uni-bochum.de

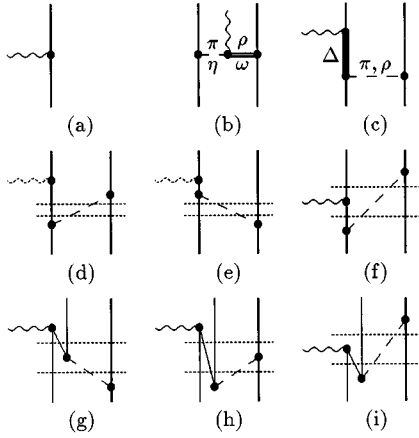


FIG. 2. Currents included in the present calculations: (a) impulse current, (b) radiative vector-meson decay currents  $VP\gamma = \rho\pi\gamma + \omega\pi\gamma + \rho\eta\gamma + \omega\eta\gamma$ , (c)  $N\Delta\gamma\pi^-$  and  $\rho$ -exchange currents, (d) and (e) wave function reorthonormalization and (f)  $NN\gamma$  meson-recoil currents, and (g) and (i)  $NN̄$ -pair creation and annihilation currents. In each of (d)–(f) and (g)–(i) we show 3 of the 12 time-ordered diagrams with the energy cuts represented by dotted lines. None of the exchange currents (b)–(i) can be obtained from Eq (1.1).

However, the above analysis is flawed for several reasons. Even within the static limit there are purely transverse currents  $\vec{J}_t$  which automatically satisfy  $\nabla \cdot \vec{J}_t = 0$ , so that current conservation places no constraints on the manifestly gauge invariant  $\rho\pi\gamma$ ,  $\omega\pi\gamma$  and  $N\Delta\gamma$  exchange currents shown in Fig. 2. None of these two-body currents can be included simply by introducing the commutators shown in Eq. (1.1), yet they all possess nonvanishing isoscalar contributions which can be important in  $pp$ -bremsstrahlung. In addition, as new experiments have succeeded in selecting kinematics that escape the consequences of the low-energy theorems [4,5] and on-shell expansions [6,7], they necessarily emphasize dynamics where the (usually dominant) nucleon-pole contributions of Figs. 1(a)–(c) are heavily suppressed by the Green’s functions accompanying the highly off-shell  $t$  matrix. As such, otherwise less important contributions gain considerable significance in the observables. This shows that the  $pp$ -bremsstrahlung dynamics involves much more than the off-shell  $t$  matrix and the impulse current, and appears to share the complexity of other observables like  $np$ -bremsstrahlung and  $n+p \Rightarrow d+\gamma$ .

A very long list of  $pp$ -bremsstrahlung calculations have been reported over the last 45 years. We will make no attempt to review them all since more recent works [8–20] already contain appropriate citation and serve to remove a number of questionable approximations. A notable exception to this trend is found in the very detailed  $r$ -space calculations reported some 25 years ago by Brown [21,22], where the rescattering amplitudes of Fig. 1(c) were retained and Eq. (1.1) was used to constrain the longitudinal meson-exchange currents. Noteworthy calculations since that time have generally been less complete, but find their merit in the application of more reliable  $NN$  interactions and the exploration of Coulomb corrections [17] and relativistic corrections to the impulse current [8,11,14,16]. Only a few of the most recent  $pp$ -bremsstrahlung calculations [1,15,19,20] attempt a sig-

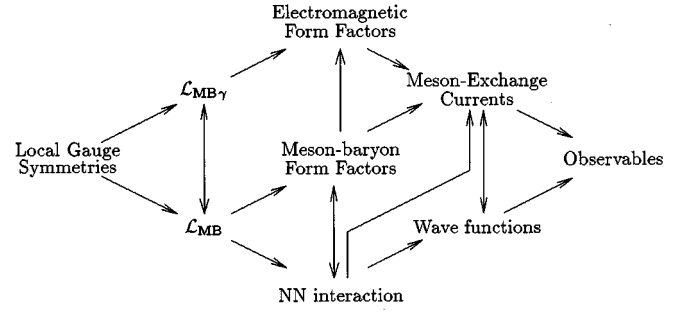


FIG. 3. In the RuhrPot effective meson field theory, meson-baryon form factors are calculated nonperturbatively and the results are used without adjustment as input for subsequent calculations of electromagnetic form factors, the  $NN$  interaction and the meson-exchange currents. Such consistency is necessary, for example, to satisfy gauge invariance (which relates the meson-exchange currents to the  $NN$  interaction) and ensure orthonormality of the wave functions (through inclusion of wave function reorthonormalization exchange currents).

nificant improvement on the standard set by Brown, although there are important technical differences in these works that we will need to consider.

In the present work we will subject the RuhrPot description of meson-baryon interactions to the test of reproducing the  $pp$ -bremsstrahlung data below the  $\pi$ -production threshold. The reasons for selecting this effective theory are the following.

(1) A microscopic definition of the strong form factors is available from nonperturbative and self-consistent calculation [23]. The results are compatible with Skyrme [24], non-topological soliton [25], and bag-model [26] calculations, and moreover, with an analysis of experiment [27].

(2) An  $NN$ -interaction model using calculated (not fitted) form factors has been constructed and gives an excellent description of the world data for the  $NN$ -scattering phase shifts [28].

(3) The extension to include meson-exchange currents in the calculation of observables introduces no free parameters whatsoever [1,15].

(4) A parameter free extension of the model to define the three-body interaction has been shown to provide an accurate description of the triton bonding energy [29].

We indicate the relationships between the form factors, the  $NN$  interaction, and the exchange currents in Fig. 3. Although such consistent calculations can (in principle) be performed for any effective meson field theory, such work has so far only been completed for the RuhrPot description and it appears that there are severe difficulties in obtaining similar consistency in other models. For example, the RuhrPot form factor calculations have been modified to adopt the coupling constants of a conventional boson-exchange  $NN$  interaction and yield results [23] which can be accurately parametrized as monopoles with typical regularization scales of  $\Lambda \sim 0.8$  GeV. While consistency demands the use of such form factors, conventional boson-exchange models require [30] artificial scales (“cutoffs”) of  $\Lambda_\pi \geq 1.3$  GeV and  $\Lambda_\rho \sim 1.8$  GeV. Such an artificial description of the meson-nucleon vertices

necessarily frustrates any attempt to obtain a realistic description of the meson-exchange currents and the  $3N$  interaction.

Coupled channel  $t$  matrices providing a nonperturbative description of all possible transitions between  $NN$ ,  $\Delta N$ , and  $\Delta\Delta$  states have been available for more than 25 years [31–33] and have already been used to calculate the  $\Delta$ -isobar contributions to  $pp$ -bremsstrahlung observables [19,20]. Under these circumstances it may appear curious that we choose to develop a perturbative description of the  $N\Delta\gamma\pi$ - and  $\rho$ -exchange currents. However, the coupled channel  $t$  matrices used in recent  $pp$ -bremsstrahlung calculations are obtained by the inconsistent combination of the Paris [34]  $NN\Rightarrow NN$  and a static limit version of the Ried-parametrized Bochum [32]  $NN\Rightarrow\Delta N$  interaction. It is therefore impossible to accurately remove the double-counted two-pion exchange amplitudes with intermediate  $N\Delta$  states, so a free parameter is introduced to permit an approximate subtraction procedure. As such, this approach discards from the outset any hope of obtaining a microscopic description and the quality of the results must be interpreted in terms of a meaningless parameter. We will later show that, even if these inconsistencies were to be resolved by fully consistent calculation, such an approach is contingent upon a reliable description of boost operators, as well as (a subset of) the relativistic meson-exchange currents that will be developed in this work.

In the present work we develop our earlier description [1,14,15] of the RuhrPot meson-baryon interactions in the  $pp$ -bremsstrahlung data below the  $\pi$ -production threshold. In [14] we included the relativistic single and rescattering impulse-current amplitudes, and in [1,15] we introduced the fully relativistic description of the radiative vector-meson decay currents and the nonrelativistic description of the  $N\Delta\gamma\pi$ - and  $\rho$ -meson-exchange currents without recourse to the soft-photon approximation. In the present work we investigate a number of important extensions. In particular, after describing our model-independent formalism in Sec. II, we provide in Sec. III the first bremsstrahlung calculations including a fully relativistic description of the wave function reorthonormalization and meson-recoil currents that are required to ensure the orthonormality of the wave functions is preserved. We also investigate the Lorentz structure of the  $NN\pi$  vertex by providing the first calculations for the purely relativistic  $NN$  pair creation and annihilation currents. We further present relativistic expressions for the  $N\Delta\gamma\pi$ - and  $\rho$ -exchange currents and identify the source of error in various approximations. Supporting calculation details are sup-

plied in the three appendices. In Sec. IV, after establishing the sensitivity of the selected  $pp$ -bremsstrahlung observables to each of these currents and concluding that a relativistic calculation of the isobar amplitudes is necessary, we compare our relativistic results with the complete data set available from the 1990 TRIUMF  $pp$ -bremsstrahlung experiment [35]. We obtain a good description of the experimental data and conclude that a large pseudoscalar admixture in the  $NN\pi$  Lagrangian is ruled out. Further conclusions and future objectives are given in Sec. V.

## II. FORMALISM

### A. Observables

We begin by presenting the model-independent expressions we require for the calculation observables for the reaction  $N+N\rightarrow N+N+\gamma$ . The  $S$  matrix from covariant perturbation theory

$$S_{fi} = \delta_{fi} - i \int d^4x \langle f | J^\mu(x) \mathcal{A}_\mu(x) | i \rangle + \dots \quad (2.1)$$

gives the probability amplitude for a transition  $|i\rangle \rightarrow |f\rangle$  as a series involving  $0, 1, \dots$  interactions where the photon field  $\mathcal{A}_\mu(x)$  couples to the hadronic current density  $J^\mu(x)$ . Since only terms with an odd number of electromagnetic interactions can contribute to the production of a single real photon, and each of these diminishes by  $\alpha \sim 1/137$ , we retain only the lowest-order contribution and define the transition amplitude as

$$(2\pi)^4 \mathcal{T}_{fi} \delta^{(4)}(P_f - P_i) = -i \int d^4x \langle f | J^\mu(x) \mathcal{A}_\mu(x) | i \rangle. \quad (2.2)$$

Following a well-trodden path, we integrate the transition amplitude over the phase space available to the final state, and divide by the incident flux, so that with plane wave normalized to a  $\delta$  function, we obtain the lab-frame differential cross section as

$$\frac{d^3\sigma}{d\Omega_3 d\Omega_4 d\theta_\gamma} = \frac{(2\pi)^{-5} \frac{1}{2} m^3}{|\vec{p}_1|} |\tilde{\mathcal{M}}_{fi}|^2 J_{ps}, \quad (2.3)$$

where, for the  $pp$ - and  $nn$ -bremsstrahlung reactions, we have

$$|\tilde{\mathcal{M}}_{fi}|^2 = \begin{cases} |\mathcal{M}_{fi}|^2 & \text{if } M_{S_i}, M_{S_f}, \lambda \text{ measured,} \\ \frac{1}{4} \sum_{S_i M_{S_i}} \sum_{S_f M_{S_f}} \sum_{\lambda=1}^2 |\mathcal{M}_{fi}|^2 & \text{if } M_{S_i}, M_{S_f}, \lambda \text{ not measured,} \end{cases} \quad (2.4)$$

and for  $np$ -bremsstrahlung we require

$$|\tilde{\mathcal{M}}_{fi}|^2 = \begin{cases} \frac{1}{2} \sum_{T_i, T_f} |\mathcal{M}_{fi}|^2 & \text{if } M_{S_i}, M_{S_f}, \lambda \text{ measured,} \\ \frac{1}{8} \sum_{T_i, T_f} \sum_{S_i M_{S_i}} \sum_{S_f M_{S_f}} \sum_{\lambda=1}^2 |\mathcal{M}_{fi}|^2 & \text{if } M_{S_i}, M_{S_f}, \lambda \text{ not measured,} \end{cases} \quad (2.5)$$

with the invariant amplitude given by

$$\mathcal{M}_{fi} = i(2\pi)^{15/2} m^{-2} [2\omega E_1 E_2 E_3 E_4]^{1/2} \mathcal{F}_{fi}. \quad (2.6)$$

We retain only the transverse polarization vectors for the real photon since, within the Gupta-Bleuler quantization formalism, the longitudinal and scalar components can be made to cancel with a gauge transformation, and therefore cannot affect the observables. The ‘‘phase-space factor’’  $J_{\text{ps}}$  appearing in Eq. (2.3) is defined for arbitrary noncoplanarity  $\Phi = (\pi + \phi_3 - \phi_4)/2$  as

$$J_{\text{ps}} = \frac{p_3^2 p_4^2}{E_3 E_4 |\cos\theta_\gamma|} \left| \frac{N}{k \sin\theta_\gamma \cos\theta_\gamma} \right|^{-1} \quad (2.7)$$

with

$$\begin{aligned} N = & (p_4 \sin\theta_4 - p_3 \sin\theta_3) [\sin(\theta_3 + \theta_4) - (\beta_3 \sin\theta_4 \\ & + \beta_4 \sin\theta_3) \cos\theta_\gamma] - k \sin^2\theta_\gamma (\beta_3 \cos\theta_4 - \beta_4 \cos\theta_3) \\ & + 2 \sin\theta_3 \sin\theta_4 \sin^2\Phi [(p_3 \cos\theta_3 - p_4 \cos\theta_4) \\ & - (p_3 \beta_3 - p_4 \beta_4) \cos\theta_\gamma], \end{aligned} \quad (2.8)$$

where we use  $\beta_i = p_i/E_i$  for laboratory-frame reaction kinematics  $p_1 + p_2 \rightarrow p_3 + p_4 + k$ . We realize that in the limit

$\theta_\gamma \rightarrow 0$ , where  $\Phi \rightarrow 0$  is guaranteed,  $N^{-1}$  possesses singularities but  $k \sin\theta_\gamma/N$  remains well defined. Our description of kinematics and phase space is the same as that reported in the detailed discussion of [36]. As such, it is sufficient to note that in [36] it was shown that  $J_{\text{ps}}$  possess a square root singularity at the kinematic limit of noncoplanarity, although in the present work we avoid the nonrelativistic simplifications discussed therein.

For the calculation of polarized observables it is convenient to denote  $d\sigma(\pm\hat{i})$  as the cross section of Eq. (2.3) measured with the beam polarized in the  $\pm\hat{i}$  direction. We choose the quantization axis as the beam direction in the lab frame, and define the vector analyzing powers as

$$A_i = \frac{d\sigma(+\hat{i}) - d\sigma(-\hat{i})}{d\sigma(+\hat{i}) + d\sigma(-\hat{i})} = \frac{\sum_{T_i T_f \lambda} \text{Tr}\{\mathcal{M}_{fi}(\vec{\sigma} \cdot \hat{i})_{[1]} \mathcal{M}_{fi}^\dagger\}}{\sum_{T_i T_f \lambda} \text{Tr}\{\mathcal{M}_{fi} \mathcal{M}_{fi}^\dagger\}}, \quad (2.9)$$

where  $i = \hat{x}, \hat{y}$ , or  $\hat{z}$  in the lab frame. Similarly, the tensor analyzing powers (sometimes called ‘‘spin-correlation coefficients’’) are given by

$$A_{ij} = \frac{d\sigma(+\hat{i}, +\hat{j}) + d\sigma(-\hat{i}, -\hat{j}) - d\sigma(+\hat{i}, -\hat{j}) - d\sigma(-\hat{i}, +\hat{j})}{d\sigma(+\hat{i}, +\hat{j}) + d\sigma(-\hat{i}, -\hat{j}) + d\sigma(+\hat{i}, -\hat{j}) + d\sigma(-\hat{i}, +\hat{j})} = \frac{\sum_{T_i T_f \lambda} \text{Tr}\{\mathcal{M}_{fi}(\vec{\sigma} \cdot \hat{i})_{[1]} (\vec{\sigma} \cdot \hat{j})_{[2]} \mathcal{M}_{fi}^\dagger\}}{\sum_{T_i T_f \lambda} \text{Tr}\{\mathcal{M}_{fi} \mathcal{M}_{fi}^\dagger\}} \quad (2.10)$$

where, for example,  $d\sigma(+\hat{i}, -\hat{j})$  is the cross section measured with the beam polarized in the  $+\hat{i}$  direction and the target polarized in the  $-\hat{j}$  direction.

## B. The Hadronic current

To obtain a microscopic definition of the invariant amplitude we compute the Fock-space matrix elements of the photon field and hadronic current densities appearing in Eq. (2.2), so that after making use of translational invariance and selecting the Lorentz-Heaviside system with natural units, Eq. (2.6) can be recast as

$$\mathcal{M}_{fi} = (2\pi)^6 m^{-2} \sqrt{E_1 E_2 E_3 E_4} \epsilon_\mu(\vec{k}, \lambda) \langle \Psi_f^{(-)} | J^\mu(0) | \Psi_i^{(+)} \rangle, \quad (2.11)$$

where the field-theoretic hadronic current is given by

$$J^\mu(x) = \partial_\nu \frac{\partial \mathcal{L}}{\partial(\partial_\nu \mathcal{A}_\mu)} - \frac{\partial \mathcal{L}}{\partial \mathcal{A}_\mu} \quad (2.12)$$

for the Lagrangian  $\mathcal{L}$  describing electromagnetic interactions with the interacting meson-baryon system. Direct calculation of Eq. (2.11) is impossible since  $|\Psi_i^{(+)}\rangle$  and  $|\Psi_f^{(-)}\rangle$  represent complete meson-baryon states and therefore involve nucleon, resonance and meson degrees of freedom to infinite order. The problem can, however, be approached with a Hamilton formalism [3] where the total Hilbert space is partitioned into meson+resonance +antinucleon vacuum and existing subspaces,

$$\mathcal{H}_\eta = \{|NN\rangle\}, \quad \mathcal{H}_\lambda = \{\text{the rest}\}. \quad (2.13)$$

We will refer to these subspaces as the  $\eta$  space, and  $\lambda$  space, respectively. Defining  $\eta$  and  $\lambda$  as operators satisfying the conventional algebra  $\eta^2 = \eta$ ,  $\lambda^2 = \lambda$  and  $\eta\lambda = \lambda\eta = 0$  and

which project out the components of  $\mathcal{H}_\eta$  and  $\mathcal{H}_\lambda$ , respectively, we apply a unitary transformation to decouple the meson-resonance vacuum and existing components of wave functions. Although this formalism makes provision for applications involving (for example) explicit meson and/or  $\Delta$  (see Appendix A) degrees of freedom in the initial and final states, we confine our present application to energies below the  $\pi$ -production threshold, so that the complete interacting meson-baryon wave function can be written as

$$|\Psi\rangle = (1+A) \frac{1}{\sqrt{1+A^\dagger A}} |\mathcal{E}\rangle, \quad (2.14)$$

where  $|\mathcal{E}\rangle$  is the two-nucleon state vector and  $A = \lambda A \eta$  is required to satisfy  $\lambda(H + [H, A] - AHA)\eta = 0$ . In particular, we can expand both  $A$  and the Hamiltonian  $H$  in powers  $n$  of the coupling constant, so that with the free-particle energy denoted as  $H_0$ , we have

$$H = H_0 + \sum_{n=1}^{\infty} H_n, \quad A = \sum_{n=1}^{\infty} A_n \quad (2.15)$$

and note that  $\eta H_1 \eta = \eta H_0 \lambda = \lambda H_0 \eta = 0$ , to obtain

$$0 = \sum_{n=1}^{\infty} \lambda \left[ H_n + [H_0, A_n] + \sum_{i=1}^{n-1} H_i A_{n-i} - \sum_{i=1}^{n-2} \sum_{j=1}^{n-i-1} A_i H_j A_{n-i-j} \right] \eta. \quad (2.16)$$

We are free to further constrain  $A$  by demanding Eq. (2.16) is satisfied at each order of  $n$ , as would be required for any perturbative application. Since  $H_0 \eta |\Psi\rangle = \mathcal{E}_i \eta |\Psi\rangle$ , where  $\mathcal{E}_i$  is the asymptotic energy of the free two-nucleon state, we obtain

$$(\mathcal{E}_i - H_0) A_n = \lambda \left[ H_n + \sum_{i=1}^{n-1} H_i A_{n-i} - \sum_{i=1}^{n-2} \sum_{j=1}^{n-i-1} A_i H_j A_{n-i-j} \right] \eta. \quad (2.17)$$

Since  $A_0 = 0$ , we have

$$A_1 = \frac{\lambda}{\mathcal{E}_i - H_0} H_1 \eta, \quad (2.18a)$$

$$A_2 = \frac{\lambda}{\mathcal{E}_i - H_0} H_2 \eta + \frac{\lambda}{\mathcal{E}_i - H_0} H_1 \frac{\lambda}{\mathcal{E}_i - H_0} H_1 \eta. \quad (2.18b)$$

Finally, with

$$H_1 = - \int \mathcal{L} d^3x \quad (2.19)$$

we observe that  $A$  is completely determined by the strong interaction Lagrangian density defining any model of interest. Combining Eqs. (2.11) and (2.14), we then obtain

$$\mathcal{M}_{fi} = (2\pi)^6 m^{-2} \sqrt{E_1 E_2 E_3 E_4} \langle \mathcal{E}_f | \epsilon_\mu(\vec{k}, \lambda) J_{\text{eff}}^\mu(0) | \mathcal{E}_i \rangle, \quad (2.20)$$

where

$$\begin{aligned} J_{\text{eff}}^\mu(0) &= \eta \frac{1}{\sqrt{1+A^\dagger A}} (1+A^\dagger) J^\mu(0) (1+A) \frac{1}{\sqrt{1+A^\dagger A}} \eta \\ &= \eta \left[ J^\mu(0) + J^\mu(0)A + A^\dagger J^\mu(0) + A^\dagger J^\mu(0)A \right. \\ &\quad \left. - \frac{1}{2} J^\mu(0)A^\dagger A - \frac{1}{2} A^\dagger A J^\mu(0) + \dots \right] \eta \end{aligned} \quad (2.21)$$

is the effective meson-baryon current density. Equation (2.21) provides a time-ordered relativistic description of the impulse- and meson-exchange currents implied by the strong interaction Lagrangian density defining any model of interest. This provides, without approximation, a noncovariant three-vector representation where all particles are confined to their mass shells and energy need not be conserved at individual vertices. An intuitive understanding of the processes embedded in the effective current density can be obtained by noting that the operator  $A$  is always associated with transitions from the  $\eta$  space into the  $\lambda$  space, so that with our present definitions,  $A$  serves to create meson+resonance+antinucleon existing states and  $A^\dagger$  serves to restore purely two-nucleon states. In the second-order expansion of this current we observe direct terms  $J$ , initial- and final-state interaction terms  $JA + A^\dagger J$ , meson-recoil terms  $A^\dagger JA$ , and wave function reorthonormalization terms  $JA^\dagger A$  and  $A^\dagger AJ$ . The wave function reorthonormalization terms result directly from the requirement that the transformation used to obtain Eq. (2.14) is unitary — or equivalently, from the fact that we insist upon working with orthonormal wave functions. This point has been discussed in considerable detail elsewhere [3].

We select a momentum-space representation and perform a  $t$ -matrix expansion of the two-nucleon wave functions according to the standard procedure. With the photon field quantized in the Gupta-Bleuler formalism, we require only the transverse polarization vectors. Since these have a vanishing time component, we require only the spacial parts of the effective current density, so that

$$\mathcal{M}_{fi} = N \vec{\epsilon}(\vec{k}, \lambda) \langle \vec{p}_3 \vec{p}_4; \alpha_f | \vec{J}_{\text{eff}}(0) | \vec{p}_1 \vec{p}_2; \alpha_i \rangle \quad (2.22a)$$

$$+ N \vec{\epsilon}(\vec{k}, \lambda) \langle \vec{p}_3 \vec{p}_4; \alpha_f | \vec{J}_{\text{eff}}(0) G_i t^{(+)} | \vec{p}_1 \vec{p}_2; \alpha_i \rangle \quad (2.22b)$$

$$+ N \vec{\epsilon}(\vec{k}, \lambda) \langle \vec{p}_3 \vec{p}_4; \alpha_f | t^{(-)\dagger} G_f \vec{J}_{\text{eff}}(0) | \vec{p}_1 \vec{p}_2; \alpha_i \rangle \quad (2.22c)$$

$$+ N \vec{\epsilon}(\vec{k}, \lambda) \langle \vec{p}_3 \vec{p}_4; \alpha_f | t^{(-)\dagger} G_f \vec{J}_{\text{eff}}(0) G_i t^{(+)} | \vec{p}_1 \vec{p}_2; \alpha_i \rangle, \quad (2.22d)$$

where  $G_i$  and  $G_f$  are  $\eta$ -space Green's functions describing the propagation of two-nucleon states and

$$N = -(2\pi)^6 m^{-2} \sqrt{E_1 E_2 E_3 E_4}. \quad (2.23)$$

TABLE I. RuhrPot parameters adopted in the present calculation. All  $NN$ -meson form factors are taken from direct calculation. For the  $\epsilon$  meson this requires a meson scale of  $\Lambda_1=0.6$  GeV, whereas all other mesons require  $\Lambda_1=0.8$  GeV. (Further details can be found in [23,28].) We adopt the experimental results  $g_{\rho\pi\gamma}=0.53$ ,  $g_{\omega\pi\gamma}=2.58$ ,  $g_{\rho\eta\gamma}=1.39$ ,  $g_{\omega\eta\gamma}=0.15$ , and  $\kappa^{is}=-0.12$ ,  $\kappa^{iv}=3.706$ . SU(6) and vector dominance indicate  $\mu_{N\Delta}=3.993$ .

$\beta$	$m_\beta$ (MeV)	$g_{NN\beta}$	$\kappa_\beta$ (GeV) $^{-2}$	$\Sigma_\beta$	${}^\kappa\Sigma_\beta$	$g_{N\Delta\beta}$
$\pi$	136.5	12.922	...	49.516	...	28.85
$\eta$	548.8	6.015	...	...	...	...
$\rho$	776.9	1.651	6.400	0.0124	28.105	20.73
$\omega$	782.4	4.945	1.088	12.379	0.4334	...
$\delta$	983.0	6.043	...	...	...	...
$\epsilon$	975.0	10.567	...	5.6911	...	...

The four terms shown in Eq. (2.22) will be referred to as direct, initial-state, final-state, and rescattering amplitudes, respectively.

### III. MODEL DEFINITION AND CALCULATION DETAILS

#### A. The RuhrPot Lagrangian

We adopt the strong-interaction Lagrangian densities,

$$\begin{aligned} \mathcal{L}_{NN\pi} &= -i g_{NN\pi} \bar{\psi} \left( \lambda \gamma^5 - (1-\lambda) \frac{1}{2m} \gamma^5 \gamma^\mu (i\partial_\mu) \right) \psi \vec{\pi} \cdot \vec{\tau}, \\ \mathcal{L}_{NN\eta} &= -\frac{g_{NN\eta}}{2m} \bar{\psi} \gamma^5 \gamma^\mu \partial_\mu \psi \eta, \\ \mathcal{L}_{NN\rho} &= -g_{NN\rho} \bar{\psi} \gamma^\mu \psi \vec{\rho}_\mu \cdot \vec{\tau}, \\ \mathcal{L}_{NN\omega} &= -g_{NN\omega} \bar{\psi} \gamma^\mu \psi \omega_\mu, \\ \mathcal{L}_{NN\delta} &= -g_{NN\delta} \bar{\psi} \psi \vec{\delta} \cdot \vec{\tau}, \\ \mathcal{L}_{NN\epsilon} &= -g_{NN\epsilon} \bar{\psi} \psi \epsilon, \\ \mathcal{L}_{N\Delta\pi} &= -\frac{g_{N\Delta\pi}}{2m} \bar{\psi}^\mu \vec{\tau}_{N\Delta} \psi \partial_\mu \vec{\pi} + \text{H.c.}, \\ \mathcal{L}_{N\Delta\rho} &= -i \frac{g_{N\Delta\rho}}{2m} \bar{\psi}^\mu \gamma^5 \gamma^\nu \vec{\tau}_{N\Delta} \psi \vec{\rho}_{\mu\nu} + \text{H.c.}, \end{aligned} \quad (3.1)$$

where  $\rho_{\mu\nu} = \partial_\mu \rho_\nu - \partial_\nu \rho_\mu$ , and we have denoted  $g_{N\Delta\rho} = \mu_{N\Delta} g_\rho$ ,  $g_{NN\rho} = (1/2)g_\rho$ , and  $g_{NN\omega} = (1/2)g_\omega$ , where  $g_\rho$  and  $g_\omega$  the strong charges for the  $\rho$  and  $\omega$  gauge fields. For the electromagnetic-interaction we use the Lorentz-Heaviside system with natural units, where the charge of the proton is defined as  $e_p = +\sqrt{4\pi\alpha}$  with  $\alpha \sim 1/137.04$ , and we adopt the Lagrangians

$$\mathcal{L}_{NN\gamma} = -e_N \bar{\psi} \gamma^\mu \psi \mathcal{A}_\mu + \frac{e_p \kappa_N}{2m} \bar{\psi} \sigma^{\mu\nu} \partial_\nu \mathcal{A}_\mu \psi,$$

$$\mathcal{L}_{PV\gamma} = -\frac{e_p g_{PV\gamma}}{2m_V} \epsilon^{\mu\nu\sigma\tau} F_{\mu\nu} \vec{\Phi}_\sigma^V \cdot \partial_\tau \vec{\Phi}^P,$$

$$\mathcal{L}_{N\Delta\gamma} = -i \frac{e_p}{2m} \mu_{N\Delta} \bar{\psi}^\mu \gamma^5 \gamma^\nu \vec{\tau}_{N\Delta}^3 \psi F_{\mu\nu} + \text{H.c.}, \quad (3.2)$$

where  $F_{\mu\nu} = \partial_\mu A_\nu - \partial_\nu A_\mu$ ,  $\vec{\Phi}^V = \vec{\rho}$  or  $\omega$ ,  $\vec{\Phi}^P = \vec{\pi}$  or  $\eta$ ,  $e_N = e_p [(1 + \tau^3)/2]$  and  $\mu_N = (1 + \kappa^{is})/2 + [(1 + \kappa^{iv})/2] \tau^3 = 1 + \kappa_N$  with  $\kappa^{is} = -0.12$  and  $\kappa^{iv} = 3.706$ .

These Lagrangians describe the bare coupling of mass renormalized fields. The form factors describing the coupling constant renormalization have been calculated [23] as a coupled set of integral equations yielding results which can be accurately parametrized as monopoles with the regularization scales shown in Table I. These renormalized couplings are implemented by replacing the Lagrangians with the vertex functions describing their dressed counterparts,

$$\begin{aligned} \Gamma_{NN\pi} &= -i g_{NN\pi} F_{NN\pi} \bar{\psi} \\ &\quad \times \left( \lambda \gamma^5 - (1-\lambda) \frac{1}{2m} \gamma^5 \gamma^\mu (i\partial_\mu) \right) \psi \vec{\pi} \cdot \vec{\tau}, \\ \Gamma_{NN\eta} &= -\frac{g_{NN\eta} F_{NN\eta}}{2m} \bar{\psi} \gamma^5 \gamma^\mu \partial_\mu \psi \eta, \\ \Gamma_{NN\rho} &= -g_{NN\rho} \bar{\psi} \left( F_{NN\rho}^{(1)} \gamma^\mu - \frac{\kappa_\rho F_{NN\rho}^{(2)}}{2m} \sigma^{\mu\nu} \partial_\nu \right) \psi \vec{\rho}_\mu \cdot \vec{\tau}, \\ \Gamma_{NN\omega} &= -g_{NN\omega} \bar{\psi} \left( F_{NN\omega}^{(1)} \gamma^\mu - \frac{\kappa_\omega F_{NN\omega}^{(2)}}{2m} \sigma^{\mu\nu} \partial_\nu \right) \psi \omega_\mu, \\ \Gamma_{NN\delta} &= -g_{NN\delta} F_{NN\delta} \bar{\psi} \psi \vec{\delta} \cdot \vec{\tau}, \Gamma_{NN\epsilon} = -g_{NN\epsilon} F_{NN\epsilon} \bar{\psi} \psi \epsilon, \\ \Gamma_{N\Delta\pi} &= -\frac{g_{N\Delta\pi} F_{N\Delta\pi}}{2m} \bar{\psi}^\mu \vec{\tau}_{N\Delta} \psi \partial_\mu \vec{\pi} + \text{H.c.}, \\ \Gamma_{N\Delta\rho} &= -i \frac{g_{NN\rho} G_{N\Delta\rho}}{2m} \frac{g_{N\Delta\pi}}{g_{NN\pi}} \bar{\psi}^\mu \gamma^5 \gamma^\nu \vec{\tau}_{N\Delta} \psi \vec{\rho}_{\mu\nu} + \text{H.c.}, \end{aligned} \quad (3.3)$$

where  $G_{N\Delta\rho} = F_{N\Delta\rho}^{(1)} + \kappa_\rho F_{N\Delta\rho}^{(2)}$  and we normalize all form factors as  $F(0) = 1$ . As in other exchange-current applications

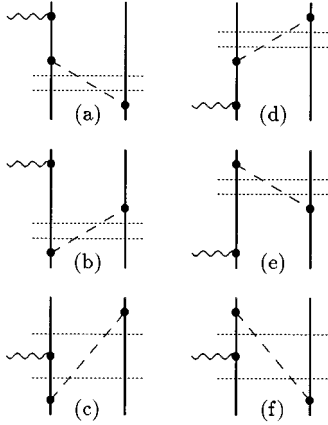


FIG. 4.  $NN\gamma$  wave function reorthonormalization and meson-recoil exchange currents. These currents are necessary to preserve the orthonormality of the initial- and final-state wave functions.

[37] the experimentally unknown values of  $g_{N\Delta\rho}=20.73$  and  $\mu_{N\Delta}=3.993$  are fixed according to SU(6) [38,39] and vector-meson dominance as

$$\mu_{N\Delta} = \mu_N^{iv} \frac{g_{N\Delta\pi}}{g_{NN\pi}}, \quad g_{N\Delta\rho} = g_{NN\rho} (1 + \kappa_\rho) \frac{g_{N\Delta\pi}}{g_{NN\pi}}, \quad (3.4)$$

where  $\mu_N^{iv} = \frac{1}{2} G_M^V(0) = 2.353$ . Note that the tensor couplings  $\kappa_\rho$  and  $\kappa_\omega$  are absent from the Lagrangians of Eq. (3.1) but appear in the dressed vertex functions of Eq. (3.3) since they are directly computed from the loop integrals appearing in the form factor calculation [23]. A similar consideration for the electromagnetic form factors is obviously not required for the real photon.

The  $NN\alpha$  properties are taken from the fit of the RuhrPot two-nucleon interaction [28] to the  $NN$ -scattering data. The form factor scales adopted in [28] were actually calculated within a nonrelativistic framework [40,41], but the recent relativistic calculation [23] has confirmed the parameterizations. We acknowledge some ambiguity in the signs of the  $PV\gamma$  coupling constants [42,43] but adopt  $g_{\rho\pi\gamma}=0.53$ ,  $g_{\omega\pi\gamma}=2.58$ ,  $g_{\rho\eta\gamma}=1.39$ , and  $g_{\omega\eta\gamma}=0.15$ , as reported in [44]. We use the experimental result  $g_{N\Delta\pi} = 28.85$ , which is consistent with the Chew-Low [45] and strong-coupling [46–48] models and, moreover, with the form factor calculations [23]. We will not fiddle with these values in order to optimize selected experimental results since this would spoil the consistency between the calculation of the meson-baryon form factors, the  $NN$  interaction and the exchange currents.

## B. Impulse and exchange currents

We describe here the impulse and meson-exchange currents  $J_{\text{eff}}$ , as required in Eq. (2.22). We adopt a partition of Hilbert spaces into meson+resonance+antinucleon vacuum and existing parts, as described in Sec. II. In the present work we confine our attention to leading-order exchange currents involving the electromagnetic coupling to the  $NN$ ,  $\bar{N}N$ ,  $PV = \rho\pi$ ,  $\omega\pi$ ,  $\rho\eta$ , and  $\omega\eta$  and  $N\Delta$  currents, so that

$$J_{\text{eff}} = J_{\text{eff}}^{NN} + J_{\text{eff}}^{\bar{N}N} + J_{\text{eff}}^{PV} + J_{\text{eff}}^{N\Delta}. \quad (3.5)$$

The effective current can therefore be derived unambiguously from Eqs. (3.2), (3.3), (2.12), (2.18), (2.19), and (2.21). Throughout we describe the momenta of a meson with mass  $m_\beta$  with

$$\begin{aligned} \vec{q}_1 &= \vec{p}_3 - \vec{p}_1, & \omega_1 &= \sqrt{\vec{q}_1^2 + m_\beta^2}, & q_1^0 &= E_3 - E_1, & Q_1^2 &= -q_1^2, \\ \vec{q}_2 &= \vec{p}_4 - \vec{p}_2, & \omega_2 &= \sqrt{\vec{q}_2^2 + m_\beta^2}, & q_2^0 &= E_4 - E_2, & Q_2^2 &= -q_2^2, \end{aligned} \quad (3.6)$$

and, denoting the nucleon and  $\Delta$ -isobar masses as  $m$  and  $m_\Delta$ , we condense our notation with

$$\begin{aligned} \vec{p}_{ik} &= \begin{cases} \vec{p}_i - \vec{k} & \text{for } i=1,2, \\ \vec{p}_i + \vec{k} & \text{for } i=3,4, \end{cases} \\ E_{ik} &= \sqrt{\vec{p}_{ik}^2 + m^2}, & \mathcal{E}_{ik} &= E_{ik} + m, \\ E_{\Delta ik} &= \sqrt{\vec{p}_{ik}^2 + m_\Delta^2}, & \mathcal{E}_{\Delta ik} &= E_{\Delta ik} + m_\Delta. \end{aligned} \quad (3.7)$$

### 1. Impulse and exchange currents with the relativistic $NN\gamma$ vertex

For the partition of Hilbert spaces defined in Sec. II B, all contributions involving a vertex where the photon couples to the nucleon current must satisfy  $\lambda J_{NN}\eta = \eta J_{NN}\lambda = 0$ , so that Eq. (3.5) requires

$$\begin{aligned} \langle \vec{p}_3 \vec{p}_4 | [J_{\text{eff}}^{NN}]^\mu | \vec{p}_1 \vec{p}_2 \rangle &= J_{NN\gamma}^\mu [1](\vec{p}_1, \vec{p}_3) \delta(\vec{p}_4 - \vec{p}_2) \\ &+ J_{NN\gamma}^\mu [2](\vec{p}_2, \vec{p}_4) \delta(\vec{p}_3 - \vec{p}_1) \\ &+ \langle \vec{p}_3 \vec{p}_4 | J_{\text{WFRR}}^\mu | \vec{p}_1 \vec{p}_2 \rangle, \end{aligned} \quad (3.8)$$

where the first two terms describe the impulse currents for nucleons 1 and 2, and the last term denotes the wave function reorthonormalization and meson-recoil currents

$$\begin{aligned} \langle \vec{p}_3 \vec{p}_4 | J_{\text{WFRR}}^\mu | \vec{p}_1 \vec{p}_2 \rangle &= -g_{\sigma\tau} \\ &\times \sum_\beta [D_{abc}^{NN\beta} J_{NN\gamma}^\mu [1](\vec{p}_{3k}, \vec{p}_3) H_{NN\beta}^\sigma [1](\vec{p}_1, \vec{p}_{3k}) H_{NN\beta}^\tau [2](\vec{p}_2, \vec{p}_4) \\ &+ D_{def}^{NN\beta} H_{NN\beta}^\sigma [1](\vec{p}_{1k}, \vec{p}_3) H_{NN\beta}^\tau [2](\vec{p}_2, \vec{p}_4) J_{NN\gamma}^\mu [1](\vec{p}_{1k}, \vec{p}_1)] + (1,3 \Rightarrow 2,4), \end{aligned} \quad (3.9)$$

where  $\beta = \pi, \eta, \rho, \omega, \delta$ , and  $\epsilon$ , and the factor  $-g_{\sigma\tau}$  resulting from the contraction of the vector-meson polarizations and all references to the Lorentz indices  $\sigma$  and  $\tau$  are to be ignored for the scalar mesons. Explicit expressions for the vertex functions  $H_{NN\beta}$  and current  $J_{NN\gamma}$  are supplied in Appendix B. The propagator functions are labeled in correspondence to Fig. 4 and are defined as

$$\begin{aligned}
D_{abc}^\beta &= \frac{1}{[E_4 - E_2 - \omega_2][E_1 - E_{3k} - \omega_2]} \\
&\quad - 1/2 \\
&\quad + \frac{1}{[E_3 - E_1 - \omega_2][E_2 - E_4 - \omega_2]} \\
&\quad - 1/2 \\
&\quad + \frac{1}{[E_3 + E_4 - E_{3k} - E_2 - \omega_2][E_1 - E_{3k} - \omega_2]}, \\
D_{def}^\beta &= \frac{1}{[E_3 - E_{1k} - \omega_2][E_2 - E_4 - \omega_2]} \\
&\quad - 1/2 \\
&\quad + \frac{1}{[E_4 - E_2 - \omega_2][E_1 - E_3 - \omega_2]} \\
&\quad - 1/2 \\
&\quad + \frac{1}{[E_3 - E_{1k} - \omega_2][E_1 + E_2 - E_{1k} - E_4 - \omega_2]}.
\end{aligned} \tag{3.10}$$

In the static limit we note that  $D_{abc}^\beta = D_{def}^\beta = 0$  so that the wave function renormalization and meson-recoil exchange

currents  $J_{\text{WFR}}^\mu$  simply vanish. The same conclusion can be reached within the soft-photon approximation in the barycentric frame.

Since we will avoid these approximations, we are forced to accept that a relativistic description of the photon coupling to the positive-frequency components of the impulse current  $J_{NN\gamma}^\mu$  necessarily leads to an effective current density  $J_{\text{eff}}$  comprising both one- and two-body operators. These two-body contributions have, to date, never been explicitly included in any of the bremsstrahlung calculations that seek to include the relativistic components of the  $NN\gamma$  vertex.

## 2. Pair currents

The sum of one-body impulse-currents  $J_{NN\gamma}^\mu$  and the wave function reorthonormalization and meson-recoil exchange currents  $J_{\text{WFR}}^\mu$  do not exhaust the requirements needed to obtain a relativistic description of the photon coupling to the nucleon current density since the off-shell nucleon comprises a linear superposition of positive and (so far neglected) negative frequency components. In the Feynman-Stückelberg approach, the negative-frequency components of the off-shell nucleon field are interpreted as antiparticles, so we are led to introduce the photon coupling to the  $N\bar{N}$ -pair creation and annihilation currents.

Within our partition of Hilbert spaces, the photon coupling to the  $N\bar{N}$ -pair creation and annihilation vertices must satisfy  $\eta J_{\bar{N}N} \eta = 0$ , so that Eq. (3.5) requires

$$\begin{aligned}
\langle \vec{p}_3 \vec{p}_4 | [J_{\text{eff}}^{\bar{N}N}]^\mu | \vec{p}_1 \vec{p}_2 \rangle &= -g_{\sigma\tau} \\
&\times \sum_{\beta} [D_{abc}^{NN\beta} H_{NN\beta}^\sigma [1](\vec{p}_1, \vec{p}_{3k}) H_{NN\beta}^\tau [2](\vec{p}_2, \vec{p}_4) J_{NN\gamma}^\mu [1](\vec{p}_{3k}, \vec{p}_3) \\
&\quad + D_{def}^{NN\beta} J_{NN\gamma}^\mu [1](\vec{p}_{1k}, \vec{p}_1) H_{NN\beta}^\sigma [1](\vec{p}_{1k}, \vec{p}_3) H_{NN\beta}^\tau [2](\vec{p}_2, \vec{p}_4)] + (1, 3 \rightleftharpoons 2, 4),
\end{aligned} \tag{3.11}$$

where  $\beta = \pi, \eta, \rho, \omega, \delta$ , and  $\epsilon$ , and the factor  $-g_{\sigma\tau}$  and all references to the Lorentz indices  $\sigma$  and  $\tau$  are to be ignored for the scalar mesons. Explicit expressions for the pair-creation and -annihilation currents  $J_{N\bar{N}\gamma}$  and  $J_{\bar{N}N\gamma}$  and all required vertex functions are described in Appendix B. The propagator functions are labeled in correspondence to Fig. 5 and are defined as

$$\begin{aligned}
D_{abc}^\beta &= \frac{1}{[-E_{3k} - E_1 - \omega_2][E_4 - E_{3k} - E_1 - E_2]} \\
&\quad + \frac{1}{[E_4 - E_2 - \omega_2][E_4 - E_{3k} - E_1 - E_2]} \\
&\quad + \frac{1}{[-E_{3k} - E_1 - \omega_2][E_2 - \omega_2 - E_4]},
\end{aligned}$$

$$\begin{aligned}
D_{def}^\beta &= \frac{1}{[E_2 - E_{1k} - E_3 - E_4][ -E_{1k} - E_3 - \omega_2]} \\
&\quad + \frac{1}{[E_2 - E_{1k} - E_3 - E_4][E_2 - \omega_2 - E_4]} \\
&\quad + \frac{1}{[E_4 - \omega_2 - E_2][ -E_{1k} - E_3 - \omega_2]}.
\end{aligned} \tag{3.12}$$

We will adopt these expressions for our numerical work. Nonetheless, it is interesting to consider the corresponding result under various approximations. If we demand energy conservation across the current matrix elements, then Eq. (3.12) reduces to



$$D_{abc}^{\beta} = \frac{-2\omega_2}{(E_3+k+E_{3k})(q_2^2-m_{\beta}^2)} \stackrel{nr}{\sim} \frac{2}{\omega_2(2m+k)} \stackrel{spa}{\sim} \frac{1}{\omega_2 m}$$

$$D_{def}^{\beta} = \frac{-2\omega_2}{(E_1-k+E_{1k})(q_2^2-m_{\beta}^2)} \stackrel{nr}{\sim} \frac{2}{\omega_2(2m-k)} \stackrel{spa}{\sim} \frac{1}{\omega_2 m}, \quad (3.13)$$

where we also provide the static-limit and soft-photon reductions. The corresponding  $\pi$ -exchange contribution under such approximations are

$$\langle \vec{p}_3 \vec{p}_4 | [J_{\text{eff}}^{\bar{N}N}]^{\mu} | \vec{p}_1 \vec{p}_2 \rangle \stackrel{nr}{\sim} \frac{\lambda e_p g_{NN\pi}^2 F_{NN\pi}^2(\vec{q}_2)}{(2\pi)^6 4m(q_2^2+m_{\pi}^2)} \vec{\sigma}_1(\vec{\sigma}_2 \cdot \vec{q}_2) \left\{ \frac{(1+\vec{\tau}_1^z)\vec{\tau}_1 \cdot \vec{\tau}_2}{2m-k} - \frac{\vec{\tau}_1 \cdot \vec{\tau}_2 (1+\tau_1^0)}{2m+k} \right\} + (1 \rightleftharpoons 2),$$

$$\langle \vec{p}_3 \vec{p}_4 | [J_{\text{eff}}^{\bar{N}N}]^{\mu} | \vec{p}_1 \vec{p}_2 \rangle \stackrel{spa}{\sim} \frac{-\lambda e_p g_{NN\pi}^2 F_{NN\pi}^2(\vec{q}_2)}{(2\pi)^6 4m^2(q_2^2+m_{\pi}^2)} \vec{\sigma}_1(\vec{\sigma}_2 \cdot \vec{q}_2) (i\vec{\tau}_1 \times \vec{\tau}_2)^3 + (1 \rightleftharpoons 2). \quad (3.14)$$

Both of these results scale linearly with the parameter  $\lambda$  controlling the admixture of ps- and pv couplings in the  $NN\pi$  Lagrangian, but the well-known isovector structure of the nonrelativistic pair currents holds only for soft photons. Since the data with which we will compare our results was planned to maximize the photon energy, we anticipate a non-negligible contribution from the isoscalar components of Eq. (3.11). This offers the possibility of studying  $\lambda$  without the complications of describing the many leading-order exchange currents that contribute to  $np$ -bremsstrahlung.

### 3. $PV\gamma$ currents

The  $\omega$  meson (782.4 MeV) decays as  $\omega \rightarrow \pi^0 \gamma$  with an 8.7% branching ratio and indicates the coupling constant of  $g_{\omega\pi\gamma}=2.58$ . As such, the  $\omega\pi\gamma$  exchange currents can be expected to make a nontrivial contribution to both the  $pp$ - and  $np$ -bremsstrahlung observables. Analogous arguments indicate that the  $\rho\pi\gamma$  contributions will be large in  $np$ -bremsstrahlung, and perhaps also of some lesser importance in  $pp$ -bremsstrahlung.

Our desire to preserve complete consistency between the form factors,  $NN$  interaction, and the exchange currents leads us to introduce all leading-order exchange currents describing the photon coupling to the decay of all vector-meson mesons present in the form factor and  $NN$ -interaction calculations. We therefore include the  $PV\gamma = \rho\pi\gamma + \omega\pi\gamma + \rho\eta\gamma + \omega\eta\gamma$  exchange currents as shown in Fig. 6. Each of these vertices satisfies  $\eta J_{\bar{p}\nu}\eta=0$ , so that after making use of Eqs. (3.2), (2.12), and (2.21), Eq. (3.5) requires

$$\langle \vec{p}_3 \vec{p}_4 | [J_{\text{eff}}^{VP}]^{\mu} | \vec{p}_1 \vec{p}_2 \rangle = \frac{\sqrt{4\omega_P(\vec{q}_1)\omega_V(\vec{q}_2)}}{(2\pi)^3 m_V [q_1^2 - m_P^2] [q_2^2 - m_V^2]}$$

$$\times H_{NNP}[1](\vec{p}_1, \vec{p}_3) \epsilon_{\nu}(\hat{q}_2, \lambda_V) H_{NNV}^{\nu}[2](\vec{p}_2, \vec{p}_4) J_{VP\gamma}^{\mu}(q_1, q_2)$$

$$+ (1,3 \rightleftharpoons 2,4), \quad (3.15)$$

where  $J_{VP\gamma}$  is given in Appendix B. We require only the three-vector current, for which the relativistic form is

$$\langle \vec{p}_3 \vec{p}_4 | \vec{J}_{\text{eff}}^{VP} | \vec{p}_1 \vec{p}_2 \rangle$$

$$= -\frac{e_p g_{VP\gamma} F_{VP\gamma} \sqrt{4\omega_P(\vec{q}_1)\omega_V(\vec{q}_2)}}{(2\pi)^3 m_V [q_1^2 - m_P^2] [q_2^2 - m_V^2]} H_{NNP}[1](\vec{p}_1, \vec{p}_3)$$

$$\times \{H_{NNV}^0[2](\vec{p}_2, \vec{p}_4)[\vec{q}_1 \times \vec{q}_2] + \vec{H}_{NNV}[2](\vec{p}_2, \vec{p}_4)$$

$$\times [(q_2)_0 \vec{q}_1 - (q_1)_0 \vec{q}_2]\} + (1,3 \rightleftharpoons 2,4). \quad (3.16)$$

We will not resort to the nonrelativistic limit, but we realize it implies  $q_1^0=q_2^0=0$ , so that we recover the well-known result for the emission of a real photon of momentum  $\vec{k}$ ,

$$\langle \vec{p}_3 \vec{p}_4 | \vec{J}_{\text{eff}}^{VP} | \vec{p}_1 \vec{p}_2 \rangle \stackrel{nr}{\sim} \frac{i e_p g_{VP\gamma} g_{NNV} g_{NNP}}{(2\pi)^6 2m_V m [q_1^2 + m_P^2] [q_2^2 + m_V^2]}$$

$$\times (\vec{\sigma}_1 \cdot \vec{q}_1)(\vec{q}_1 \times \vec{q}_2)(\vec{\tau}_1)_P(\vec{\tau}_2)_V + (1,3 \rightleftharpoons 2,4), \quad (3.17)$$

where  $(\vec{\tau}_1)_P(\vec{\tau}_2)_V = \vec{\tau}_1 \cdot \vec{\tau}_2$ ,  $\vec{\tau}_1^0$ ,  $\vec{\tau}_2^0$  and 1 for the  $\rho\pi\gamma$ ,  $\omega\pi\gamma$ ,  $\rho\eta\gamma$  and  $\omega\eta\gamma$ , currents, respectively.

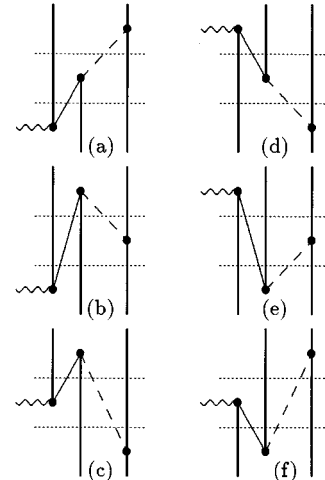


FIG. 5.  $\bar{N}N$  pair creation and annihilation meson-exchange currents. These currents are necessary for a relativistic description of the  $NN$  vertex.

#### 4. $N\Delta\gamma$ exchange currents

All contributions involving a vertex where the photon couples to the  $N\Delta$  current must satisfy  $\eta J_{\Delta N} \eta = \eta J_{N\Delta} \eta = 0$ , so that Eq. (3.5) requires

$$\begin{aligned} & \langle \vec{p}_3 \vec{p}_4 | \vec{J}_{\text{eff}}^{N\Delta} | \vec{p}_1 \vec{p}_2 \rangle = -g_{\sigma\tau} \\ & \times \sum_{\beta} [D_{abc}^{\beta} \vec{J}_{N\Delta\gamma}[1](\vec{p}_{3k}, \vec{p}_3) H_{\Delta N\beta}^{\sigma}[1](\vec{p}_1, \vec{p}_{3k}) H_{NN\beta}^{\tau}[2](\vec{p}_2, \vec{p}_4) \\ & + D_{def}^{\beta} H_{N\Delta\beta}^{\sigma}[1](\vec{p}_{1k}, \vec{p}_1) \vec{J}_{\Delta N\gamma}[1](\vec{p}_1, \vec{p}_{1k}) H_{NN\beta}^{\tau}[2](\vec{p}_2, \vec{p}_4)] + (1,3 \rightleftharpoons 2,4), \end{aligned} \quad (3.18)$$

where  $\beta = \vec{\pi}$  or  $\vec{\rho}$  and the factor  $-g_{\sigma\tau}$  resulting from the contraction of the  $\rho$ -meson polarizations and all references to the Lorentz indices  $\sigma$  and  $\tau$  are to be ignored for  $\beta = \pi$ . Explicit expressions for the vertex functions and currents shown in Eq. (3.18) are supplied in Appendix B. We ignore all negative-frequency resonance contributions. The propagator functions are labeled in correspondence to Fig. 7 and are defined in analogy to the previous sections. Using energy conservation for the current matrix elements and introducing the  $\Delta$  decay width  $\Gamma_{\Delta}$  via [47,48]  $E_{\Delta k} \rightarrow E_{\Delta k} - i\Gamma_{\Delta}/2$ , the propagators reduce to

$$\begin{aligned} D_{abc}^{\beta} &= \frac{2\omega_2}{(q_2^2 - m_{\beta}^2)(E_3 + k - E_{\Delta 3k} + i\Gamma_{\Delta}/2)}, \\ D_{def}^{\beta} &= \frac{2\omega_2}{(q_2^2 - m_{\beta}^2)(E_1 - k - E_{\Delta 1k} + i\Gamma_{\Delta}/2)}. \end{aligned} \quad (3.19)$$

An exact calculation of Eq. (3.18) can be achieved with the use of the vertex functions and currents given in Appendix B. However, at present there exists some uncertainty in the coupling constants  $g_{N\Delta\rho}$  and  $\mu_{N\Delta}$ , so that such a rigorous procedure is of limited interest. We simplify matters by dropping terms of order  $p^2/(E+m)^2$  beyond leading order, an approximation which does not involve any  $p/m$  expansion and should be accurate to within a few percent at energies

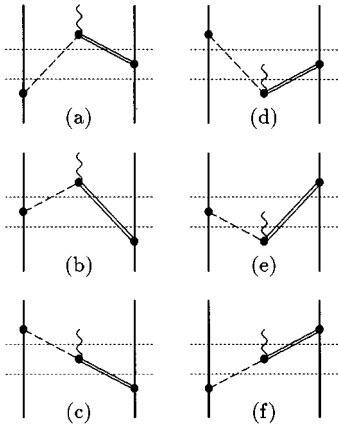


FIG. 6.  $VP\gamma = \rho\pi\gamma + \omega\pi\gamma + \rho\eta\gamma + \omega\eta\gamma$  exchange currents. When energy is conserved across these current matrix elements, the time-ordered graphs exactly sum to form the corresponding Feynman diagrams.

below the  $\pi$ -production threshold. This is surely adequate for the first-order  $S_{fi}$  matrix described in Sec. II A.

We introduce the condensed notation

$$\begin{aligned} \vec{\mathcal{P}}_i &= \frac{\vec{p}_i}{\mathcal{E}_i}, \quad \vec{\mathcal{P}}_{\Delta ki} = \frac{\vec{p}_{ik}}{\mathcal{E}_{\Delta ik}}, \quad \vec{\mathcal{Q}}_{ij} = \vec{p}_{ik} \left( \frac{E_j}{m_{\Delta}} \right) - \vec{p}_j, \\ \vec{\mathcal{H}}_i &= \vec{p}_{ik} \left( \frac{2E_{\Delta ik} - E_i}{m_{\Delta}} \right) - \vec{p}_i, \\ \vec{\mathcal{L}}_i &= \left( \frac{\vec{p}_{ik}}{\mathcal{E}_{\Delta ik}} - \frac{\vec{p}_i}{\mathcal{E}_i} \right) (m + m_{\Delta}), \quad i = 1, 2, 3, 4, \end{aligned} \quad (3.20)$$

and proceed to calculate separately the contributions from  $\pi$  and  $\rho$  exchange,

$$\vec{J}_{\text{eff}}^{N\Delta} = \vec{J}_{\text{eff}}^{N\Delta}(\pi) + \vec{J}_{\text{eff}}^{N\Delta}(\rho). \quad (3.21)$$

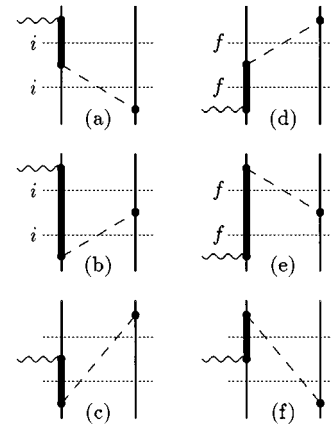


FIG. 7.  $N\Delta\gamma$   $\pi$ - and  $\rho$ -meson exchange currents. In the RuhrPot model the  $\pi$ -exchange contributions represent the largest of the two-body currents in  $pp$ -bremsstrahlung but the  $\rho$ -exchange contributions are very small. When energy is conserved across these current matrix elements, the time-ordered graphs exactly sum to form the corresponding Feynman diagrams.

### 5. $N\Delta\gamma$ $\pi$ -exchange currents

The effective current describing the excitation of intermediate  $\Delta$  isobars through  $\pi$  exchange can now be obtained from Eqs. (3.18) and Appendix B. For the real photon, we require only the spacial current, which takes the form

$$\begin{aligned} \langle \vec{p}_3 \vec{p}_4 | \vec{J}_{\text{eff}}^{N\Delta}(\pi) | \vec{p}_1 \vec{p}_2 \rangle = & N_1 \vec{\sigma}_2 \cdot (\vec{\mathcal{P}}_4 - \vec{\mathcal{P}}_2) [2\tau_2^3 - (i\tau_1 \times \tau_2)^3] [(\vec{\mathcal{H}}_1 + \vec{\mathcal{L}}_1) \times \vec{Q}_{13} + (i\vec{\sigma}_1 \times \vec{Q}_{13}) \vec{\mathcal{L}}_1 + i\vec{\sigma}_1 \times [(\vec{\mathcal{H}}_1 - \vec{\mathcal{L}}_1) \times \vec{Q}_{13}] \\ & - 2i\vec{\sigma}_1 [(\vec{\mathcal{H}}_1 - \vec{\mathcal{L}}_1) \cdot \vec{Q}_{13}] + N_3 \vec{\sigma}_2 \cdot (\vec{\mathcal{P}}_4 - \vec{\mathcal{P}}_2) [2\tau_2^3 + (i\tau_1 \times \tau_2)^3] [(\vec{\mathcal{H}}_3 + \vec{\mathcal{L}}_3) \times \vec{Q}_{31} - (i\vec{\sigma}_1 \times \vec{Q}_{31}) \\ & \times \vec{\mathcal{L}}_3 - i\vec{\sigma}_1 \times [(\vec{\mathcal{H}}_3 - \vec{\mathcal{L}}_3) \times \vec{Q}_{31}] + 2i\vec{\sigma}_1 [(\vec{\mathcal{H}}_3 - \vec{\mathcal{L}}_3) \cdot \vec{Q}_{31}] + (1,3 \rightleftharpoons 2,4), \end{aligned} \quad (3.22)$$

where

$$N_0 = \frac{-ie_p \mu_{N\Delta} g_{N\Delta} g_{NN\pi}}{(2\pi)^6 72m^2} \left[ \frac{\mathcal{E}_1 \mathcal{E}_2 \mathcal{E}_3 \mathcal{E}_4}{16E_1 E_2 E_3 E_4} \right]^{1/2} \frac{F_{NN\pi}(Q_2^2) F_{N\Delta\pi}(Q_2^2)}{\omega_\pi(\vec{q}_2^2)}, \quad N_1 = \frac{N_0 \mathcal{E}_{\Delta 1k} D_{def}^\pi}{2E_{\Delta 1k}}, \quad N_3 = \frac{N_0 \mathcal{E}_{\Delta 3k} D_{abc}^\pi}{2E_{\Delta 3k}}. \quad (3.23)$$

We will adopt Eq. (3.22) for our numerical applications and use it to consider the merit of various approximations that are conventionally adopted to recover a simplified operator structure.

The first level of approximation involves taking the static limit and ignoring the  $N$ - $\Delta$  mass difference in Eq. (3.20). We call this the *vertex static limit* approximation and note that it is equivalent to casting Eq. (3.22) as

$$\begin{aligned} \langle \vec{p}_3 \vec{p}_4 | \vec{J}_{\text{eff}}^{N\Delta}(\pi) | \vec{p}_1 \vec{p}_2 \rangle = & (N_1 + N_3) \frac{(\vec{\sigma}_2 \cdot \vec{q}_2)}{2m} [4\tau_2^3 \vec{q}_2 - (i\vec{\tau}_1 \times \vec{\tau}_2)^3 (i\vec{\sigma}_1 \times \vec{q}_2)] \times \vec{k} \\ & - 2(N_1 - N_3) \frac{(\vec{\sigma}_2 \cdot \vec{q}_2)}{2m} [\tau_2^3 (i\vec{\sigma}_1 \times \vec{q}_2) - (i\vec{\tau}_1 \times \vec{\tau}_2)^3 \vec{q}_2] \times \vec{k} + (1,3 \rightleftharpoons 2,4). \end{aligned} \quad (3.24)$$

The substantial simplification results primarily because the vertex static limit approximation indicates  $\mathcal{H}_1 = \mathcal{L}_1 = -\vec{k}$ , and  $\mathcal{H}_3 = \mathcal{L}_3 = \vec{k}$ , so that all operator structures involving  $\mathcal{H}_i - \mathcal{L}_i$  immediately vanish. However, if we consider the static limit with the more reasonable approximation  $m_\Delta \sim (4/3)m$ , then we find

$$\begin{aligned} \mathcal{H}_1 + \mathcal{L}_1 & \sim -\frac{17}{8}\vec{k} - \frac{1}{24}\vec{p}_1, & \mathcal{H}_1 - \mathcal{L}_1 & \sim -\frac{3}{8}\vec{k} + \frac{13}{24}\vec{p}_1, \\ \mathcal{H}_3 + \mathcal{L}_3 & \sim \frac{17}{8}\vec{k} - \frac{1}{24}\vec{p}_3, & \mathcal{H}_3 - \mathcal{L}_3 & \sim \frac{3}{8}\vec{k} + \frac{13}{24}\vec{p}_3, \end{aligned} \quad (3.25)$$

so that the  $\mathcal{H}_i + \mathcal{L}_i$  terms surviving in the vertex static limit are rather well approximated, but the neglected  $\mathcal{H}_i - \mathcal{L}_i$  terms are poorly represented.

The second level of approximation involves casting the complete expression in the static limit. This is the approximation we adopted in earlier work [1,15]. At the small momentum transfers relevant to the present numerical applica-

tion, this *complete static limit* approximation will differ little from the vertex static limit and, if we further set  $\Gamma_\Delta = 0$  and drop the form factor dependence, it is equivalent to casting Eq. (3.22) in the simpler form

$$\begin{aligned} \langle \vec{p}_3 \vec{p}_4 | \vec{J}_{\text{eff}}^{N\Delta}(\pi) | \vec{p}_1 \vec{p}_2 \rangle = & \frac{-ie_p \mu_{N\Delta} g_{N\Delta} g_{NN\pi}}{(2\pi)^6 36m^3} \\ & \times (\vec{\sigma}_2 \cdot \vec{q}_2) \left\{ \frac{4(m_\Delta - m)\vec{q}_2 + 2|\vec{k}|(i\vec{\sigma}_1 \times \vec{q}_2)}{[(m_\Delta - m)^2 - |\vec{k}|^2](\vec{q}_2^2 + m_\pi^2)} \tau_2^3 \right. \\ & \left. + \frac{(m_\Delta - m)(i\vec{\sigma}_1 \times \vec{q}_2) + 2|\vec{k}|\vec{q}_2}{[(m_\Delta - m)^2 - |\vec{k}|^2](\vec{q}_2^2 + m_\pi^2)} (i\vec{\tau}_1 \times \vec{\tau}_2)^3 \right\} \times \vec{k} \\ & + (1,3 \rightleftharpoons 2,4). \end{aligned} \quad (3.26)$$

The third and final approximation we consider is obtained by neglecting the  $|\vec{k}|$  dependence in the complete static limit description of the baryon propagators. This *soft-photon approximation* gives the conventional description [37] of the  $N\Delta\gamma(\pi)$  exchange current for the radiation of a photon of momentum  $\vec{k}$ ,

$$\begin{aligned} \langle \vec{p}_3 \vec{p}_4 | \vec{J}_{\text{eff}}^{N\Delta}(\pi) | \vec{p}_1 \vec{p}_2 \rangle &= \frac{-ie_p \mu_{N\Delta} g_{N\Delta\pi} g_{NN\pi}}{(2\pi)^6 36m^3(m_\Delta - m)} \\ &\times (\vec{\sigma}_2 \cdot \vec{q}_2) \left\{ \frac{4\tau_2^3 \vec{q}_2}{\vec{q}_2^2 + m_\pi^2} + \frac{(i\vec{\tau}_1 \times \vec{\tau}_2)^3 (i\vec{\sigma}_1 \times \vec{q}_2)}{\vec{q}_2^2 + m_\pi^2} \right\} \times \vec{k} \\ &+ (1,3 \rightleftharpoons 2,4). \end{aligned} \quad (3.27)$$

We anticipate that this result will differ from the complete static limit whenever the photon energy is comparable to the  $N$ - $\Delta$  mass difference.

### 6. $N\Delta\gamma$ $\rho$ -exchange currents

Within the soft-photon approximation, it is well known [37] that the  $N\Delta\gamma$   $\rho$ -exchange currents are small compared to the corresponding  $\pi$ -exchange currents, although the de-

structive interference between the two makes it necessary to include both. In the present work, we anticipate the  $\rho$ -exchange contributions to be less important than in other works because the RuhrPot model suggests a very weak  $NN\rho$  coupling constant. [In particular, RuhrPot [28] uses  $g_{NN\rho}^2/4\pi = 0.2169$  and  $\kappa_\rho = 6.4$ , whereas (for example) Bonn B [49] adopts  $g_{NN\rho}^2/4\pi = 0.92$  and  $\kappa_\rho = 6.1$ .]

Since the  $N\Delta\gamma$   $\rho$ -exchange currents are expected to be small, we proceed by taking the *vertex static limit* approximation from the outset. In complete analogy to the derivation of Eq. (3.22), we obtain

$$\vec{J}_{\text{eff}}^{N\Delta}(\rho) = \vec{J}_{\text{eff}}^{N\Delta}(\rho; E) + \vec{J}_{\text{eff}}^{N\Delta}(\rho; M), \quad (3.28)$$

where

$$\begin{aligned} \langle \vec{p}_3 \vec{p}_4 | \vec{J}_{\text{eff}}^{N\Delta}(\rho; E) | \vec{p}_1 \vec{p}_2 \rangle &= \{ [4N_E^{(+)}(\vec{p}_2 + \vec{p}_4) \times \vec{q}_2 + 2N_E^{(-)}i\sigma_1 \times [(\vec{p}_2 + \vec{p}_4) \times \vec{q}_2]] \tau_2^3 \\ &+ [2N_E^{(-)}(\vec{p}_2 + \vec{p}_4) \times \vec{q}_2 + N_E^{(+)}i\sigma_1 [(\vec{p}_2 + \vec{p}_4) \times \vec{q}_2]] (i\vec{\tau}_1 \times \vec{\tau}_2)^3 \} \times \vec{k} + (1,3 \rightleftharpoons 2,4) \end{aligned} \quad (3.29)$$

and

$$\begin{aligned} \langle \vec{p}_3 \vec{p}_4 | \vec{J}_{\text{eff}}^{N\Delta}(\rho; M) | \vec{p}_1 \vec{p}_2 \rangle &= \{ [4N_M^{(+)}[(i\sigma_2 \times \vec{q}_2) \times \vec{q}_2] - 2N_M^{(-)}(\sigma_1 \times [(\sigma_2 \times \vec{q}_2) \vec{q}_2])] \tau_2^3 \\ &+ (2N_M^{(-)}[(i\sigma_2 \times \vec{q}_2) \vec{q}_2] - N_M^{(+)}[\sigma_1 \times [(\sigma_2 \times \vec{q}_2) \times \vec{q}_2]]) (i\vec{\tau}_1 \times \vec{\tau}_2)^3 \} \times \vec{k} + (1,3 \rightleftharpoons 2,4) \end{aligned} \quad (3.30)$$

with

$$N_0 = \frac{\text{SU}(6) e_p g_{NN\rho}^2 G_M^V(0) G_M^{N\Delta\rho}(Q_2^2)}{100m^3(2\pi)^6 \omega_\rho(\vec{q}_2)}$$

$$N_E^{(+)} = N_0 F_{NN\rho}^{(1)}(Q_2^2) [D_{def}^\rho + D_{abc}^\rho], \quad N_M^{(+)} = N_0 [F_{NN\rho}^{(1)}(Q_2^2) + \kappa_\rho F_{NN\rho}^{(2)}(Q_2^2)] [D_{def}^\rho + D_{abc}^\rho],$$

$$N_E^{(-)} = N_0 F_{NN\rho}^{(1)}(Q_2^2) [D_{def}^\rho - D_{abc}^\rho], \quad N_M^{(-)} = N_0 [F_{NN\rho}^{(1)}(Q_2^2) + \kappa_\rho F_{NN\rho}^{(2)}(Q_2^2)] [D_{def}^\rho - D_{abc}^\rho],$$

(3.31)

where we normalize  $G_M^{N\Delta\rho}(0) = 1 + \kappa_\rho$  and adopt the propagators  $D^\rho$  of Eq. (3.19). The *complete static limit* and *soft-photon* approximations follow in analogy to the procedures used to develop Eqs. (3.26) and (3.27), the latter resulting in

$$\begin{aligned} \langle \vec{p}_3 \vec{p}_4 | \vec{J}_{\text{eff}}^{N\Delta}(\rho; E) | \vec{p}_1 \vec{p}_2 \rangle &= \frac{4N_0(1 + \kappa_\rho)}{m_\Delta - m} \left\{ \frac{4\tau_2^3(\vec{p}_4 + \vec{p}_2) \times \vec{q}_2}{\vec{q}_2^2 + m_\rho^2} - \frac{(\vec{\tau}_1 \times \vec{\tau}_2)^3 \vec{\sigma}_1 \times [(\vec{p}_4 + \vec{p}_2) \times \vec{q}_2]}{\vec{q}_2^2 + m_\rho^2} \right\} \times \vec{k} \\ &+ (1 \rightleftharpoons 2), \end{aligned} \quad (3.32a)$$

$$\begin{aligned} \langle \vec{p}_3 \vec{p}_4 | \vec{J}_{\text{eff}}^{N\Delta}(\rho; M) | \vec{p}_1 \vec{p}_2 \rangle &= \frac{4N_0(1 + \kappa_\rho)^2}{m_\Delta - m} \left\{ \frac{4\tau_2^3[(i\vec{\sigma}_2 \times \vec{q}_2) \times \vec{q}_2]}{\vec{q}_2^2 + m_\rho^2} - \frac{(\vec{\tau}_1 \times \vec{\tau}_2)^3 [\vec{\sigma}_1 \times [(i\vec{\sigma}_2 \times \vec{q}_2) \times \vec{q}_2]]}{\vec{q}_2^2 + m_\rho^2} \right\} \times \vec{k} \\ &+ (1 \rightleftharpoons 2), \end{aligned} \quad (3.32b)$$

where  $\vec{J}_{\text{eff}}^{N\Delta}(\rho; M)$  is the conventional result, and  $\vec{J}_{\text{eff}}^{N\Delta}(\rho; E)$  is an additional piece (resulting from the convection current part of the  $NN\rho$  vertex) which is usually ignored on the basis that it is smaller than  $\vec{J}_{\text{eff}}^{N\Delta}(\rho; M)$  by a factor of about  $1 + \kappa_\rho \sim 7$ .

### C. Direct, single and rescattering amplitudes

A model-independent expression for the complete invariant amplitude was given in Eq. (2.22), where we developed a decomposition into the four terms describing direct, single (i.e., initial and final state), and rescattering amplitudes shown in Fig. 1. The left-hand side of Eq. (2.22) is defined by the model-independent expressions of Eqs. (2.2) and (2.6), and is Lorentz invariant by construction. However, since the right-hand side of Eq. (2.22) is determined by a model-dependent calculation, there can be no *a priori* guarantee that each of the direct, single, and rescattering amplitudes are individually Lorentz invariant unless the wave functions are calculated in a manifestly covariant formalism [61].

Since the wave functions are usually constructed from an  $NN$ -interaction  $t$  matrix that is defined only in the barycentric frame, and two distinct barycentric frames appear in Eq. (2.22), we cast the entire expression into the (maximally symmetric) average barycentric frame, so that the momenta satisfy

$$\text{A frame: } \vec{p}_1 + \vec{p}_2 - \frac{1}{2}\vec{k} = 0 = \vec{p}_3 + \vec{p}_4 + \frac{1}{2}\vec{k} \quad (3.33)$$

and we acknowledge that a formal solution of the initial, final, and rescattering amplitudes requires the application of boost operators [50–53].

In the following we will make use of the fact that the effective current operator of Eq. (3.5) is totally symmetric under interchange of particles 1 and 2. As such, we obtain in an arbitrary frame,

$$\begin{aligned} & \langle \vec{p}_3 \vec{p}_4; (s_1 s_2) S_f; (t_1 t_2) T_f | J_{\text{eff}} | \vec{p}_1 \vec{p}_2; (s_1 s_2) S_i; (t_1 t_2) T_i \rangle \\ &= \langle \vec{p}_4 \vec{p}_3; (s_2 s_1) S_f; (t_2 t_1) T_f | J_{\text{eff}} | \vec{p}_2 \vec{p}_1; (s_2 s_1) S_i; (t_2 t_1) T_i \rangle \\ &= \langle \vec{p}_4 \vec{p}_3; (s_1 s_2) S_f; (t_1 t_2) T_f | J_{\text{eff}} | \vec{p}_2 \vec{p}_1; (s_1 s_2) S_i; (t_1 t_2) T_i \rangle \\ & \quad \times (-1)^{(S_i + S_f + T_i + T_f)}. \end{aligned} \quad (3.34)$$

Denoting  $|\alpha\rangle = |(s_1 s_2) S; (t_1 t_2) T\rangle$ , we define the antisymmetrized states as

$$|\widetilde{\vec{p}_1 \vec{p}_2}; \alpha\rangle = \frac{1}{\sqrt{2}} \{ |\vec{p}_1 \vec{p}_2; \alpha\rangle - (-1)^{(S+T)} |\vec{p}_2 \vec{p}_1; \alpha\rangle \}. \quad (3.35)$$

It is easy to see that parity conservation is consistent with the Fermi statistics requirement  $L+S+T=\text{odd}$  in the barycentric frame.

#### 1. Direct amplitudes

The direct amplitudes appearing in Eq. (2.22a) can be simplified with use of Eqs. (3.34) and (3.35) to give

$$\begin{aligned} \mathcal{M}_{fi}^D &= N \vec{\epsilon}(\vec{k}, \lambda) \cdot [ \langle \vec{p}_3 \vec{p}_4; \alpha_f | \vec{J}_{\text{eff}} | \vec{p}_1 \vec{p}_2; \alpha_i \rangle \\ & \quad - (-1)^{(S_i + T_i)} \langle \vec{p}_3 \vec{p}_4; \alpha_f | \vec{J}_{\text{eff}} | \vec{p}_2 \vec{p}_1; \alpha_i \rangle ], \end{aligned} \quad (3.36)$$

where  $N$  is defined in Eq. (2.23) and  $\vec{J}_{\text{eff}}$  is given by Eq. (3.5). However, momentum conservation demands that the direct terms cannot involve the one-body part of the effective current density, so in the present numerical results we include the photon coupling to  $NN$  currents with recoil and wave function renormalization currents,  $N\bar{N}$  creation and annihilation currents,  $\rho\pi\gamma$ ,  $\omega\pi\gamma$ ,  $\rho\eta\gamma$ , and  $\omega\eta\gamma$  exchange currents,  $\Delta N$  currents with  $\pi$  and  $\rho$  exchange, as described by Eqs. (3.9), (3.11), (3.16), (3.22), (3.29), and (3.30).

#### 2. Single-scattering amplitudes

The initial-state interaction amplitudes appearing in Eq. (2.22b) are given by

$$\begin{aligned} \mathcal{M}_{fi}^I &= N \vec{\epsilon}(\vec{k}, \lambda) \cdot \langle \widetilde{\vec{p}_3 \vec{p}_4}; \alpha_f | \vec{J}_{\text{eff}}(0) G_i t^{(+)} | \widetilde{\vec{p}_1 \vec{p}_2}; \alpha_i \rangle \\ &= N \vec{\epsilon}(\vec{k}, \lambda) \cdot \sum_{\alpha} \int \int d\vec{p}'_1 d\vec{p}'_2 \langle \vec{p}_3 \vec{p}_4; \alpha_f | \vec{J}_{\text{eff}}(0) | \vec{p}'_1 \vec{p}'_2; \alpha \rangle \\ & \quad \times \langle \widetilde{\vec{p}'_1 \vec{p}'_2}; \alpha | G_i t^{(+)} | \widetilde{\vec{p}_1 \vec{p}_2}; \alpha_i \rangle. \end{aligned} \quad (3.37)$$

A formal specification of this amplitude follows by inserting the full effective current density of Eq. (3.5) and defining boost the operators needed to cast the  $t$  matrix in the initial-state barycentric frame. None of the bremsstrahlung calculations known to us has attempted either of these tasks. Instead, the current has been truncated to include only one-body contributions and boost operators are ignored under the assumption that the part of the invariant amplitude resulting from initial-state correlations alone is itself individually Lorentz invariant.

The first approximation could be removed with a straightforward application of the expressions provided in earlier sections, but since we anticipate the impulse current to be significantly larger than the summed exchange currents, our present numerical applications share the conventional approximation of retaining only the impulse current in the single-scattering amplitudes. The second approximation will be justified in Sec. IV A, where we provide a perturbative analysis that indicates the  $NN\gamma$  impulse-current contributions to the single-scattering terms are close to invariant under Lorentz transformation into the barycentric frames.

We therefore cast the initial-state correlation amplitudes into the initial-state barycentric frame, where

$$\text{I frame: } \vec{p}_1 + \vec{p}_2 = 0 = \vec{p}_3 + \vec{p}_4 + \vec{k}, \quad (3.38)$$

so that Eq. (2.22b) becomes, with the kinematical notation of Eq. (3.7),

$$\begin{aligned}
\mathcal{M}_{fi}^I &= N\vec{\epsilon}(\vec{k}, \lambda) \cdot \sum_{\alpha} \langle \alpha_f | \vec{J}_{NN\gamma}[1](\vec{p}_{3k}, \vec{p}_3) | \alpha \rangle \\
&\quad \times \frac{\langle \vec{p}_{3k}; \alpha | t^{(+)} | \vec{p}_1; \alpha_i \rangle}{2E_1 - 2E_{3k} + i\eta} \\
&\quad + N\vec{\epsilon}(\vec{k}, \lambda) \cdot \sum_{\alpha} \langle \alpha_f | \vec{J}_{NN\gamma}[2](\vec{p}_{4k}, \vec{p}_4) | \alpha \rangle \\
&\quad \times \frac{\langle \vec{p}_3; \alpha | t^{(+)} | \vec{p}_1; \alpha_i \rangle}{2E_1 - 2E_3 + i\eta}, \tag{3.39}
\end{aligned}$$

where we have denoted  $\langle \vec{p}', -\vec{p}'; \alpha_f | t^{(+)} | \vec{p}, -\vec{p}; \alpha_i \rangle = \langle \vec{p}'; \alpha_f | t^{(+)} | \vec{p}; \alpha_i \rangle$ . In complete analogy, we cast the final-state correlation amplitudes into the final-state barycentric frame, where

$$F \text{ frame: } \vec{p}_1 + \vec{p}_2 - \vec{k} = 0 = \vec{p}_3 + \vec{p}_4 \tag{3.40}$$

so that Eq. (2.22c) becomes

$$\begin{aligned}
\mathcal{M}_{fi}^F &= N\vec{\epsilon}(\vec{k}, \lambda) \cdot \sum_{\alpha} \frac{\langle \vec{p}_3; \alpha_f | t^{(-)\dagger} | \vec{p}_{1k}; \alpha \rangle}{2E_3 - 2E_{1k} + i\eta} \\
&\quad \times \langle \alpha | \vec{J}_{NN\gamma}[1](\vec{p}_1, \vec{p}_{1k}) | \alpha_i \rangle \\
&\quad + N\vec{\epsilon}(\vec{k}, \lambda) \cdot \sum_{\alpha} \frac{\langle \vec{p}_3; \alpha_f | t^{(-)\dagger} | \vec{p}_1; \alpha \rangle}{2E_3 - 2E_1 + i\eta} \\
&\quad \times \langle \alpha | \vec{J}_{NN\gamma}[2](\vec{p}_2, \vec{p}_{2k}) | \alpha_i \rangle. \tag{3.41}
\end{aligned}$$

Simple kinematics establishes that the radiation of a real photon implies an off-shell  $t$  matrix, so that we are free to immediately take the limits  $\eta \rightarrow 0$  in Eqs. (3.39) and (3.41).

### 3. Rescattering amplitudes

From the results of impulse approximation calculations [9,10,14] we already know that the impulse contributions to the rescattering amplitudes constitute a correction of  $\leq 15\%$  to the corresponding single-scattering amplitudes, so for simplicity we neglect from the outset all two-body currents in the rescattering amplitudes of Eq. (2.22d). Hence, in the  $A$  frame of Eq. (3.33) we obtain

$$\begin{aligned}
\mathcal{M}_{fi}^R &= N\vec{\epsilon} \sum_{\alpha\alpha'} \int \int d\vec{p}'_1 d\vec{p}'_2 \delta^{(3)}(\vec{p}'_1 + \vec{p}'_2 - \vec{p}_1 - \vec{p}_2) \\
&\quad \times \{ \langle \vec{p}_3, \vec{p}_4; \alpha_f | t^{(-)\dagger} G_f | \vec{p}'_{1k}, \vec{p}'_2; \alpha_b \rangle \langle \alpha' | \vec{J}_{NN\gamma}[1](\vec{p}'_1, \vec{p}'_{1k}) | \alpha \rangle \langle \vec{p}'_1, \vec{p}'_2; \alpha_a | G_i t^{(+)} | \vec{p}_1, \vec{p}_2; \alpha_i \rangle \\
&\quad + \langle \vec{p}_3, \vec{p}_4; \alpha_f | t^{(-)\dagger} G_f | \vec{p}'_1, \vec{p}'_{2k}; \alpha_b \rangle \langle \alpha' | \vec{J}_{NN\gamma}[2](\vec{p}'_2, \vec{p}'_{2k}) | \alpha \rangle \langle \vec{p}'_1, \vec{p}'_2; \alpha_a | G_i t^{(+)} | \vec{p}_1, \vec{p}_2; \alpha_i \rangle \}. \tag{3.42}
\end{aligned}$$

The initial- and final-state barycentric frames differ by the photon momentum, so that no frame can be found where both  $t$  matrices are expressed in their barycentric frame. We therefore introduce a boost operator  $\chi$  satisfying [50–53]

$$\begin{aligned}
|\vec{p}_a, \vec{p}_b\rangle &= \{1 - i\chi(\vec{\mathcal{P}})\} | \vec{p} \rangle | \vec{\mathcal{P}} \rangle + \mathcal{O}(1/m^4), \\
\vec{p} &= \frac{1}{2}(\vec{p}_a - \vec{p}_b), \quad \vec{\mathcal{P}} = (\vec{p}_a + \vec{p}_b). \tag{3.43}
\end{aligned}$$

Equation (3.42) is manifestly symmetric under interchange of particles 1 and 2. However, for computation purposes, it proves convenient to make use of Eqs. (3.34), (3.35), and (3.43) to formally reexpress Eq. (3.42) in terms of the photon coupling only to nucleon 1,

$$\begin{aligned}
\mathcal{M}_{fi}^R &= 2N(-1)^{(S_f + S_i + T_f + T_i)} \sum_{\alpha, \alpha'} \vec{\epsilon} \cdot \int d\vec{p} \langle \vec{p}_3 + \frac{1}{4}\vec{k}; \alpha_f | [1 + i\chi(-\vec{k}/2)] t^{(-)\dagger} G_f [1 - i\chi(-\vec{k}/2)] | \vec{p} + \frac{1}{4}\vec{k}; \alpha' \rangle \\
&\quad \times \langle \alpha' | \vec{J}_{NN\gamma}[1](-\vec{p} - \vec{k}/2, -\vec{p} + \vec{k}/2) | \alpha \rangle \langle \vec{p} - \frac{1}{4}\vec{k}; \alpha | [1 + i\chi(+\vec{k}/2)] G_i t^{(+)} [1 - i\chi(+\vec{k}/2)] | \vec{p}_1 - \frac{1}{4}\vec{k}; \alpha_i \rangle, \tag{3.44}
\end{aligned}$$

where, since the  $t$  matrix conserves spin and isospin, the sums over the intermediate-state quantum numbers ( $\alpha = S, M_S, T, M_T$ ) are restricted such that  $S = S_i$ ,  $S' = S_f$ ,  $T = T_i$ ,  $T' = T_f$  with conserved isospin projection  $M_T$ . For reasons already indicated in the discussion of the single-scattering amplitudes, the boost operators can be neglected in the present work. A recipe for performing the numerical integration over the pole structures of Eq. (3.44) is given in Appendix C.

## IV. RESULTS AND DISCUSSION

### A. Impulse contributions

In the present work we are primarily interested to investigate a consistent calculation of the dominant isoscalar meson-exchange currents in  $pp$ -bremsstrahlung. An important precursor to this lies in establishing that the well-known discrepancy between impulse approximation calculations and experimental data cannot be resolved by selecting a different

(phase-equivalent)  $NN$  interaction. Although a qualitative similarity exists between the results of recent impulse approximation calculations for  $pp$ -bremsstrahlung observables [8–14,16,18] the calculation differences are generally not confined to the differing  $NN$  potentials. Some of these calculations describe the photon coupling to the one-body current via a Foldy-Wouthuysen transformations [8,12,13,16,18] or direct Pauli reduction [10,11,14], whereas others adopt a static limit description [9]. Some include the rescattering amplitudes of Fig. 1(c) [9–11,14,18] whereas others do not [8,12,13,16]. Further differences are found in the use of relativistic or nonrelativistic two-nucleon propagators and/or the application of (guessed) off-shell minimal relativity factors [10,11].

We avoid all of these uncertainties by presenting the results of calculations that are identical apart from the definition of the potential used to generate the  $t$ -matrix elements. We also extend the list of commonly compared potentials to include the Bonn [49], Paris [34], Nijmegen [54], and Ruhr-Pot [28]. For the present comparisons we adopt the impulse approximation, so that the effective current density developed in Sec. III B reduces to the sum of (one-body) impulse currents,  $\vec{J}_{\text{eff}} \sim \vec{J}_{NN\gamma}[1] + \vec{J}_{NN\gamma}[2]$ , as defined in Appendix B, and is therefore common to all potentials. As such, we retain initial-state, final-state, and rescattering amplitudes with the two-nucleon Green's functions described by the relativistic Lippmann-Schwinger propagators. Partial waves are summed to  $J_{\text{max}}=8$  and no form of soft-photon approximation is adopted at any stage.

In Fig. 8 we compare such calculations with the TRIUMF coplanar  $pp$ -bremsstrahlung data at  $E_{\text{lab}}=280$  MeV [35]. The cross section geometries are selected to sample both small and large proton emission angles. The analyzing power geometry is selected on the basis that it is the result most different from zero, and therefore presumably the most reliably measured. Some differences exist between our analyzing power results and those reported elsewhere [11], primarily due to differences in the rescattering calculation, as discussed in Appendix C. The essential conclusion here is that impulse approximation calculations using Bonn B, Nijmegen, Paris, and RuhrPot wave functions are almost indistinguishable, but exhibit a collective discrepancy with experiment. Given that the purpose of this experiment was to distinguish the predictions of such potentials, the differences between theory and experiment are large.

The final task remaining here is to establish that the impulse current contributions to the single-scattering amplitudes given in Eqs. (3.39) and (3.41) can be accurately described without boost operators. This approximation is common to all momentum-space bremsstrahlung calculations known to us, yet it appears to have never been verified. Some authors [10,11,20] have sought a solution to the problem by arguing that the nonrelativistic  $t$ -matrix can be made Lorentz invariant simply by attaching “minimal relativity” factors [62], so that the Lippmann-Schwinger (LS) equation can be cast in a form that is apparently identical to the Blankenbecler-Sugar (BbS) equation. However, although both of these integral equations describe the  $NN$  interaction in ladder approximation, they are not formally identical because the LS kernel is constructed in a time-ordered (noncovariant) relativistic framework, whereas the BbS kernel rep-

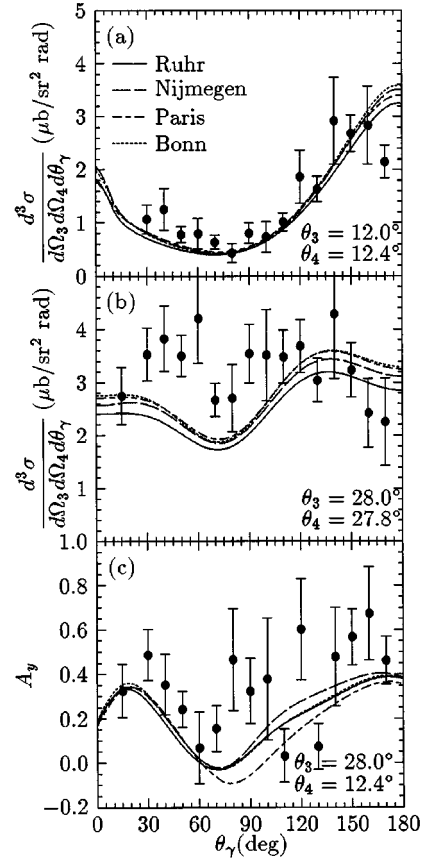


FIG. 8. Comparison of impulse approximation calculations using Ruhr, Nijmegen, Paris, and Bonn potentials and coplanar  $pp$ -bremsstrahlung data at  $E_{\text{lab}}=280$  MeV. The differences between the model results are smaller than their collective discrepancy with experiment.

resents one of an infinite number of arbitrary three-dimensional reductions of the covariant Bethe-Salpeter (BS) equation. As such, the Lippmann-Schwinger  $t$  matrix with minimal relativity factors should not be confused with a covariant definition of the  $NN$  interaction [61]. The most serious flaw in the use of minimal relativity factors is, however, that the off-shell factors are completely unknown and must be simply guessed [62]. We regard this procedure as unreasonably arbitrary, particularly since the guessed minimal relativity factors contradict the well-known form of the two-nucleon boost operators [50–53].

Since the  $t$  matrix is defined in the conventional way as  $t=V+VGt$  but is available only in the barycentric frame, we consider the arbitrary-frame perturbative reduction of these amplitudes by constructing a toy-model one-boson exchange  $NN$  interaction as

$$\begin{aligned} \langle \vec{p}'_1, \vec{p}'_2 | V | \vec{p}_1, \vec{p}_2 \rangle \\ = \frac{1}{2} \sum_{\beta} \eta H_{NN\beta}[1](\vec{p}_1, \vec{p}'_1) \lambda \left[ \frac{1}{\mathcal{E}_i - H_0} + \frac{1}{\mathcal{E}_f - H_0} \right] \\ \times \lambda H_{NN\beta}[2](\vec{p}_2, \vec{p}'_2) \eta + (1 \Rightarrow 2), \end{aligned} \quad (4.1)$$

where  $\beta=\pi, \eta, \rho$  and  $\omega$ , and  $H_{NN\beta}[i]$  is the interaction energy for a meson coupling to nucleon  $i$ , as defined in Appendix B. In Fig. 9 we present the results including only

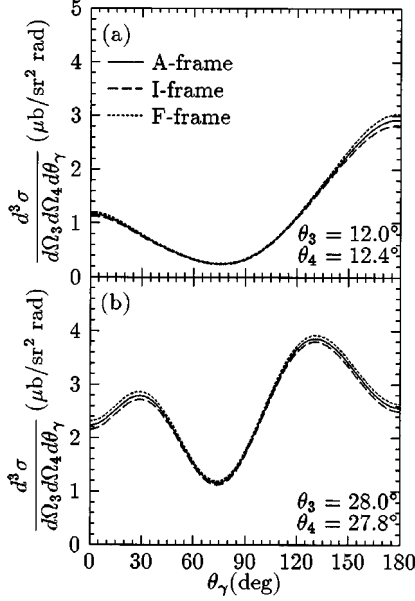


FIG. 9. Initial- and final-state interaction amplitudes in impulse approximation when the  $t$  matrix is replaced with a toy-model boson exchange potential and evaluated in the A, I, and F frames. This justifies the neglect of boost operators in the present work.

the initial- and final-state interaction amplitudes when the RuhrPot  $t$  matrix is replaced with our toy  $NN$  interaction, the complete expression being cast into the A, I and F frames of Eqs. (3.33), (3.38), and (3.40). We find that the neglect of boost operators represents an error of about 3% or less. We conclude that Eqs. (3.39) and (3.41) are essentially exact descriptions of the impulse contributions to the single-scattering amplitudes. As such, the application of minimal relativity factors [10,11,20] may need to be reconsidered.

### B. Exchange currents and the relativistic $NN\gamma$ vertex

In Sec. III B we showed that a relativistic description of the part of the effective current operator involving the photon coupling to the nucleon current comprises not only the impulse current, but also two-body contributions from the meson-recoil, wave function reorthonormalization, and pair currents. Although relativistic corrections to one-body  $NN\gamma$  currents have received considerable attention in recent  $pp$ -bremsstrahlung works [8,11–13], the two-body contributions remain to be investigated.

The wave function reorthonormalization and meson-recoil contributions are not expected to be individually small, but in Sec. III B we recalled [3] that their nonrelativistic limits cancel exactly, leaving only purely relativistic effects in the  $pp$ -bremsstrahlung observables. In the present numerical applications we retain these contributions in the spirit of exploring the relativistic aspects of the  $NN\gamma$  currents.

By far the most interesting aspect of the relativistic  $NN\gamma$  currents is found in the different manifestations of the  $N\bar{N}$  creation and annihilation pair currents given by various Dyson-equivalent chiral Lagrangians. In particular, the simplest meson-theoretic Lagrangian satisfying partially conserved axial-vector currents (PCAC) and the chiral commutation relations is the renormalizable  $\sigma$  model, for which the nucleon-meson interactions are of the form

$$\mathcal{L} = -g\bar{\psi}[\sigma + i\gamma^5\vec{\tau}\cdot\vec{\pi}']\psi. \quad (4.2)$$

With a chiral transformation  $\psi \rightarrow (1 + \vec{\xi}^2)^{-1/2} \exp[i\gamma^5\vec{\tau}\cdot\vec{\pi}']\psi$ , Weinberg [55] showed that, for a suitably constrained  $\vec{\xi}$  and redefined pion fields  $\vec{\pi} = (2m/g)\vec{\xi}$ , the Lagrangian transforms to give  $NN\pi$  and  $NN\pi\pi$  interactions with

$$\mathcal{L}_{pv} = -\frac{g}{2m}\bar{\psi}\left[1 + \frac{g^2\vec{\pi}^2}{4m^2}\right] \times \left[\gamma^5\gamma^\mu\vec{\tau}\cdot\partial_\mu\vec{\pi} + \frac{g}{2m}\vec{\tau}\cdot(\vec{\pi}\times\partial_\mu\vec{\pi})\right]\psi. \quad (4.3)$$

Similarly, the chiral transformation  $\psi \rightarrow (1 + \vec{\xi}^2)^{-1/2} \exp[i(g/2m)\vec{\tau}\cdot(\vec{\pi}'\times\vec{\xi})]\psi$  has been shown by Wess and Zumino [56] to yield  $NN\pi$  and  $NN\pi\pi$  interactions with

$$\mathcal{L}_{ps} = -\frac{g}{2m}\bar{\psi}\left[1 + \frac{g^2\vec{\pi}^2}{4m^2}\right]\left[i\gamma^5\vec{\tau}\cdot\vec{\pi} - \frac{g}{2m}\vec{\pi}^2\right]\psi. \quad (4.4)$$

In an elegant summary of these chiral Lagrangians, Gross [57] noted that both  $\mathcal{L}_{ps}$  and  $\mathcal{L}_{pv}$  give the correct  $\pi$ - $N$  scattering lengths and that the  $NN\pi\pi$  interactions have  $\rho$  and  $\sigma$  quantum numbers.

Our immediate interest lies in the pseudovector (pv) and pseudoscalar (ps)  $NN\pi$  couplings, both of which are included via the hybrid form of the  $NN\pi$  Lagrangian we adopt in Eq. (3.3) with  $0 \leq \lambda \leq 1$ . It is a trivial exercise to show that the  $\pi$  coupling to the positive-frequency components of the nucleon current described in Eq. (3.3) is independent of  $\lambda$ , so that nonrelativistic calculations cannot differentiate the ps and pv couplings. In relativistic applications  $\lambda=0$  is commonly preferred, presumably because the presence of the derivative in the pv-coupling provides for the gauge coupling of a photon to the  $NN\pi$  vertex, so that the purely isovector nonrelativistic seagull exchange currents can be included even when the microscopic structure of the  $NN\pi$  form factor is ignored. However, there are no formal arguments to rule out  $\lambda \neq 0$  and the subject is still under investigation [58,59].

In Fig. 10 we examine the relativistic  $NN\gamma$  currents in  $pp$ -bremsstrahlung by comparing the results of calculations with RuhrPot wave functions which neglect (IA) or retain (IA+MEXC) the wave function reorthonormalization, meson-recoil, and  $N\bar{N}$  pair-creation and annihilation currents with purely pv-type ( $\lambda=0$ ) and ps-type ( $\lambda=1$ )  $NN\pi$  couplings.

The first observation is the most important one:  $\lambda$  can be determined by  $pp$ -bremsstrahlung experiments. This is surely the cleanest probe of the Lorentz structure of the  $NN\pi$  vertex yet considered. We reserve our prediction for  $\lambda$  until we have included the other exchange currents given in Sec. III.

A secondary observation, which we anticipated in [14], is that the two-body contributions are small for  $\lambda=0$ . In particular, the  $\lambda=0$   $NN\gamma$  MEXC contributions to the cross sec-



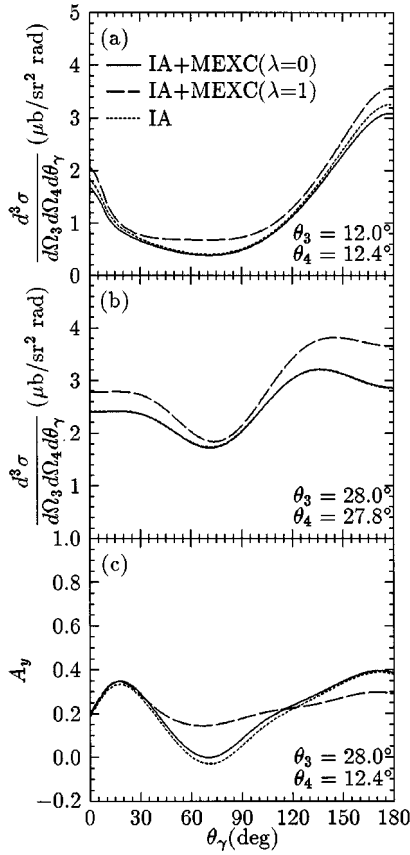


FIG. 10. RuhrPot results in impulse approximation (IA) as in Fig 8 compared to corresponding results when the wave function reorthonormalization, meson-recoil, and  $NN$ -pair currents (IA+MEXC) are included with pseudovector ( $\lambda=0$ ) or pseudoscalar ( $\lambda=1$ )  $NN\pi$  interactions.  $\lambda$  can be determined from  $pp$ -bremsstrahlung experiments.

tion at (LEP)  $\theta_3=28.0^\circ$  and (HEP)  $\theta_4=27.8^\circ$  are almost entirely negligible. However, the effects are visible in the analyzing powers, as well as in the cross section at  $\theta_3=12.0^\circ$  and  $\theta_4=12.4^\circ$ , the latter being reduced at  $\theta_\gamma=0^\circ$  and  $180^\circ$  by 0.14 and 0.17  $\mu\text{b}/\text{sr}^2/\text{rad}$  (i.e., 5% and 8%), respectively. While these effects are certainly small, they are already comparable to the model differences shown in Fig. 8.

### C. Radiative vector-meson decay currents

In Fig. 11 we compare the results of calculations using RuhrPot wave functions and the relativistic impulse current which either neglect (IA) or retain (IA+VP $\gamma$ ) the relativistic  $\rho\pi\gamma$ ,  $\omega\pi\gamma$ ,  $\rho\eta\gamma$ , and  $\omega\eta\gamma$  exchange currents [42,43]. The RuhrPot contributions are uniformly small, although we observe a reduction in the cross section at (LEP)  $\theta_3=12.0^\circ$  and (HEP)  $\theta_4=12.4^\circ$  at  $\theta_\gamma=20^\circ$  by about 0.1  $\mu\text{b}/\text{sr}^2/\text{rad}$  (i.e., 10%).

We have used the fully relativistic expressions of Eq. (3.16) for the numerical applications of Fig. 11, but to identify the dominant behavior of these exchange currents it is sufficient to consider only the static limit, neglect the  $\omega$ - and  $\rho$ -meson mass difference and neglect the  $\eta$ -meson contributions altogether. In the nonrelativistic limit, this allows us to write

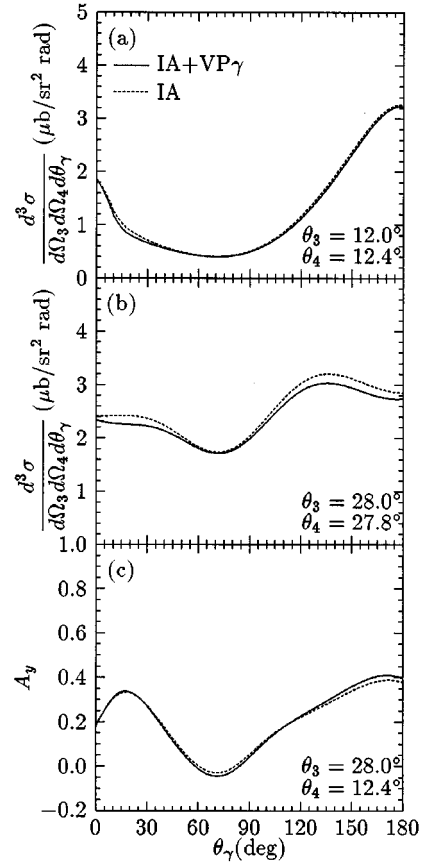


FIG. 11. RuhrPot results in impulse approximation (IA) as in Fig 8 compared to corresponding results when the VP $\gamma = \rho\pi\gamma + \omega\pi\gamma + \rho\eta\gamma + \omega\eta\gamma$  exchange currents (IA+VP $\gamma$ ) are included. The RuhrPot model has relatively weak  $NN\rho$  and  $NN\omega$  couplings, so these exchange currents are small, but comparable to the model differences shown in Fig. 8.

$$\begin{aligned} \langle \vec{p}_3 \vec{p}_4 | \vec{J}_{\text{eff}}^{\rho\pi} | \vec{p}_1 \vec{p}_2 \rangle^{nr} &\sim g_{\rho\pi\gamma} g_{NN\rho} [\hat{J}(\vec{q}_1, \vec{q}_2) + \hat{J}(\vec{q}_2, \vec{q}_1)] \vec{\tau}_1 \cdot \vec{\tau}_2, \\ \langle \vec{p}_3 \vec{p}_4 | \vec{J}_{\text{eff}}^{\omega\pi} | \vec{p}_1 \vec{p}_2 \rangle^{nr} &\sim g_{\omega\pi\gamma} g_{NN\omega} [\hat{J}(\vec{q}_1, \vec{q}_2) + \hat{J}(\vec{q}_2, \vec{q}_1)] \vec{\tau}_1^z, \end{aligned} \quad (4.5)$$

where

$$\hat{J}(\vec{q}_1, \vec{q}_2) = \frac{ie_p g_{NN\pi} (\vec{\sigma}_1 \cdot \vec{q}_1) (\vec{q}_1 \times \vec{q}_2)}{(2\pi)^6 2m_V m [\vec{q}_1^2 + m_\pi^2] [\vec{q}_2^2 + m_V^2]}. \quad (4.6)$$

Since  $g_{NN\pi}$ ,  $g_{\rho\pi\gamma}$ , and  $g_{\omega\pi\gamma}$  are essentially fixed by experiment, the freedom in the vector-meson decay exchange currents is limited to the model-dependent values adopted for the experimentally unknown coupling constants  $g_{NN\rho}$  and  $g_{NN\omega}$ . We have adopted the RuhrPot  $NN$ -interaction values of  $g_{NN\rho}=1.65$  and  $g_{NN\omega}=4.95$ , and note that these values are consistent with the broken SU(3) requirement  $g_{NN\omega}^2/g_{NN\rho}^2=9$ . The matrix elements of both isopin operators in Eq. (4.5) reduce to unity in  $pp$  bremsstrahlung, so that the  $\omega\pi\gamma$  contribution completely dominates the vector-meson decay current contributions and the corresponding  $\rho\pi\gamma$  currents are some 15 times smaller.

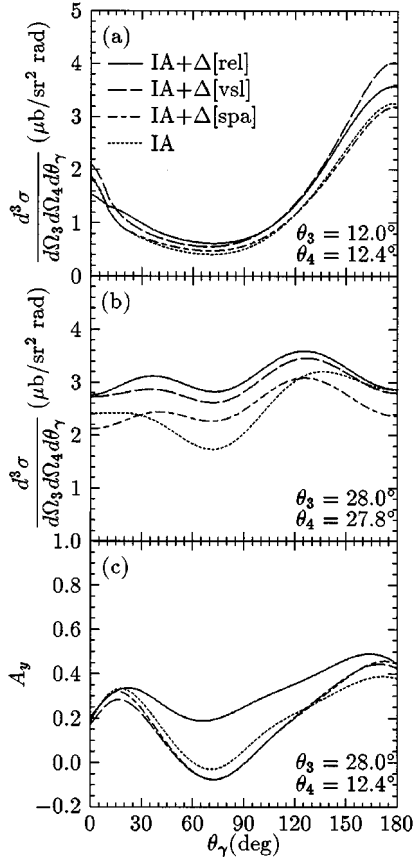


FIG. 12. RuhrPot results in impulse approximation (IA) as in Fig 8 compared to corresponding results with relativistic (rel), vertex-static limit (VSL), and soft-photon approximation (SPA)  $N\Delta\gamma$   $\pi$ - and  $\rho$ -exchange currents. A relativistic description of the  $N\Delta\gamma$  exchange currents is necessary.

The magnitude of each  $PV\gamma$  exchange current is, of course, dependent on the choice of  $NN$  interaction. For example, the Bonn B model requires  $g_{NN\rho}=3.36$  and  $g_{NN\omega}=17.5$ , so that  $g_{NN\omega}^2/g_{NN\rho}^2=27$ , which severely contradicts the broken  $SU(3)$  prediction of 9. Although the  $\rho\pi\gamma$  and  $\omega\pi\gamma$  exchange currents have never been included in Bonn model calculations for bremsstrahlung observables, it is easy to see that these currents alone would be, respectively, more than 4 and 12 times larger than the corresponding results of the present calculation.

#### D. $\Delta$ -isobar currents

In Fig. 12 we compare the results of calculations using RuhrPot wave functions and the relativistic impulse current which either neglect (IA) or retain (IA+ $\Delta$ ) the relativistic  $N\Delta\gamma$   $\pi$ - and  $\rho$ -exchange currents, as prescribed by the relativistic (rel), vertex-static limit (VSL), and soft-photon approximation (SPA) expressions developed in Sec. III B. We do not show results for the complete static limit since these results turn out to be almost indistinguishable from the vertex static limit. In Fig. 13 we decompose the contributions to the relativistic  $N\Delta\gamma$  currents into  $\pi$ - and  $\rho$ -exchange contributions. Collectively, these figures show that the RuhrPot description of the  $N\Delta\gamma$  exchange currents are very large and

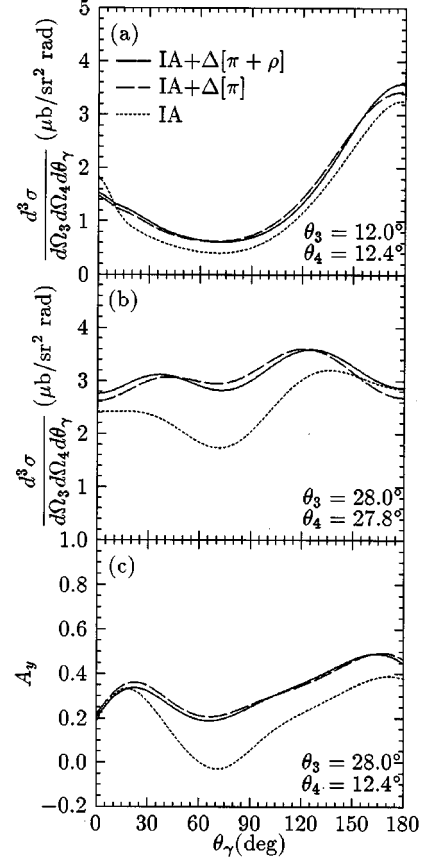


FIG. 13. RuhrPot results in impulse approximation (IA) as in Fig 8 compared to corresponding results with relativistic  $N\Delta\gamma$  exchange currents including  $\pi+\rho$  exchange ( $\pi+\rho$ ) and ( $\pi$ ) exchange ( $\pi$ ) only. The RuhrPot model has a relatively weak  $NN\rho$  coupling, so that the  $\rho$ -exchange contribution to the  $N\Delta\gamma$  currents is small.

require a relativistic description, but that the  $\rho$ -exchange contribution is comparatively small.

#### E. Comparison of exchange currents

In Fig. 14 we examine the individual contributions of each of the one- and two-body currents developed in the previous sections with the complete effective current of the present work. We observe that the  $N\Delta\gamma$  exchange currents are substantially larger than all other contributions and we recall from Fig. 13 that, in the RuhrPot description, these are completely dominated by the  $\pi$ -exchange contributions. We observe minor but non-negligible contributions from the  $VP\gamma$  currents, and we recall from Sec. IV C that the magnitude of these contributions is essentially determined by the  $NN\omega$  coupling constant in the  $NN$  interaction.

#### F. Comparison with experiment

In Figs. 15–18 we compare results of calculations using RuhrPot wave functions and the relativistic impulse current which either neglect (IA) or retain (IA+MEXC) all of the relativistic meson-exchange currents developed in the present work. These include the wave function reorthonormalization and meson-recoil currents, the  $N\bar{N}$  creation and annihilation pair currents [for both ( $\lambda=0$ ) pv and ( $\lambda=1$ ) ps

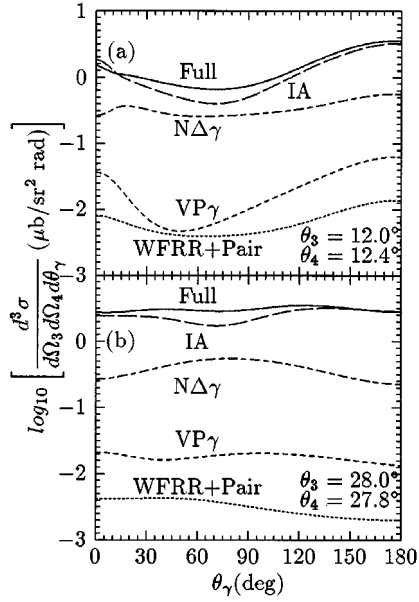


FIG. 14. Contributions from individual currents to the cross section. These are (IA) = impulse current including initial, final, and rescattering correlations, ( $N\Delta\gamma$ ) with summed  $\pi$  and  $\rho$  exchange, ( $VP\gamma$ ) =  $\rho\pi\gamma + \omega\pi\gamma + \rho\eta\gamma + \omega\eta\gamma$ , (WFRR+pair) =  $NN\gamma$  wave function reorthonormalization and meson recoil and  $\bar{N}N$ -pair creation and annihilation currents with  $\lambda=0$ . The full line denotes the sum of all these currents (with interferences).

$NN\pi$ -couplings], the  $\rho\pi\gamma$ ,  $\omega\pi\gamma$ ,  $\rho\eta\gamma$ , and  $\omega\eta\gamma$  exchange currents and the  $N\Delta\gamma$  currents with  $\pi$ - and  $\rho$ -exchange contributions. We observe that the sensitivity to the admixture of ps ( $\lambda=1$ ) and pv ( $\lambda=0$ ) couplings survives when the currents are consistently combined.

The inclusion of the relativistic exchange currents can be seen to provide a reasonable description of the cross section data in Figs. 15 and 16, but Figs. 17 and 18 show that a persistent discrepancy with experiment remains for small  $\theta_3$  and large  $\theta_4$ . The impulse approximation results for the cross section data give  $\chi^2_{\text{ir}}/\text{datum} = 5.8$ , whereas the complete exchange current calculations with ps and pv  $NN\pi$  couplings giving  $\chi^2_{\text{ps}}/\text{datum} = 6.1$  and  $\chi^2_{\text{pv}}/\text{datum} = 4.7$ , respectively. Moreover, Figs. 15 and 16 shows that adopting a ps  $NN\pi$  coupling produces structure in the cross section that is simply absent in the data. As such, the present calculations indicate that the data favors  $\lambda \sim 0$ , although Figs. 17 and 18 show that some of the most serious discrepancies with ex-

periment cannot be resolved in terms of the  $NN\pi$  coupling alone.

The importance of our conclusions on the Lorentz structure of the  $NN\pi$  vertex are contingent on a reliable data set, so we vigorously stress the need for more precise measurements of all observables where the ps and pv couplings give very different results.

### G. Some problems with nonperturbative descriptions

Strong interaction transitions between  $NN$ ,  $\Delta N$ , and  $\Delta\Delta$  states can be described non-perturbatively with a coupled channel  $t$  matrix [31–33] and indeed have already been used to calculate  $pp$ -bremsstrahlung observables [19,20]. Under these circumstances it may appear curious that we have chosen to present a perturbative description of such amplitudes as meson-exchange currents. There are, however, a number of difficulties in applications of these coupled channel  $t$  matrices, the most serious of which appears to arise from the inconsistencies that exist between the Paris [34]  $NN \rightleftharpoons NN$  and the Ried parametrized version of the static-limit Bochum [31–33]  $\Delta N \rightleftharpoons NN$  interaction. In particular, the conflicting definitions of the  $NN\pi$  and  $N\Delta\pi$  coupling constants and form factors makes it impossible to reliably remove the double-counted  $NN \rightleftharpoons NN$  amplitudes involving intermediate  $N\Delta$  states, so that a free parameter is introduced to simulate the necessary subtraction. Any specification of the two-body currents would suffer a similar ambiguity. Finally, the assumed Lorentz invariance of the  $NN \rightleftharpoons \Delta N$  transition  $t$  matrices remains to be investigated.

This leads us to consider a generalization of our formalism to obtain a fully consistent and microscopic description of the nonperturbative transitions between the  $NN$ ,  $\Delta N$ , and  $\Delta\Delta$  states. More precisely, we will identify two minimum requirements of such an approach that appear to have been neglected to date.

Recalling from Sec. II B the freedom to choose any desired partition of the total Hilbert space, we now modify our earlier choice so that the  $\Delta$  degrees of freedom are included in the  $\eta$  space. (Details can be found in Appendix A.) Within this approach, the leading-order contributions involve not only the  $NN\gamma$  impulse, wave function reorthonormalization and meson-recoil terms, but also  $N\Delta\gamma$  initial- and final-state correlation terms and  $N\Delta\gamma$  wave function reorthonormalization and meson-recoil terms, as shown in Fig. 19. Our earlier specification of the  $NN\gamma$  one- and two-body currents remains unchanged and will not be further discussed here. The additional leading-order contributions involving  $\Delta$  isobars are given by

$$\begin{aligned}
 & \langle \vec{p}_3 \vec{p}_4 | \vec{J}_{11}^{N\Delta} | \vec{p}_1 \vec{p}_2 \rangle = -g_{\sigma\tau} \\
 & \times \sum_{\beta} [D_1^{\beta} H_{N\Delta\beta}^{\sigma}[1](\vec{p}_{1k}, \vec{p}_3) \vec{J}_{\Delta N\gamma}[1](\vec{p}_1, \vec{p}_{1k}) H_{NN\beta}^{\tau}[2](\vec{p}_2, \vec{p}_4) \\
 & + D_3^{\beta} \vec{J}_{N\Delta\gamma}[1](\vec{p}_{3k}, \vec{p}_3) H_{\Delta N\beta}^{\sigma}[1](\vec{p}_1, \vec{p}_{3k}) H_{NN\beta}^{\tau}[2](\vec{p}_2, \vec{p}_4)] + (1,3 \rightleftharpoons 2,4), \quad (4.7)
 \end{aligned}$$

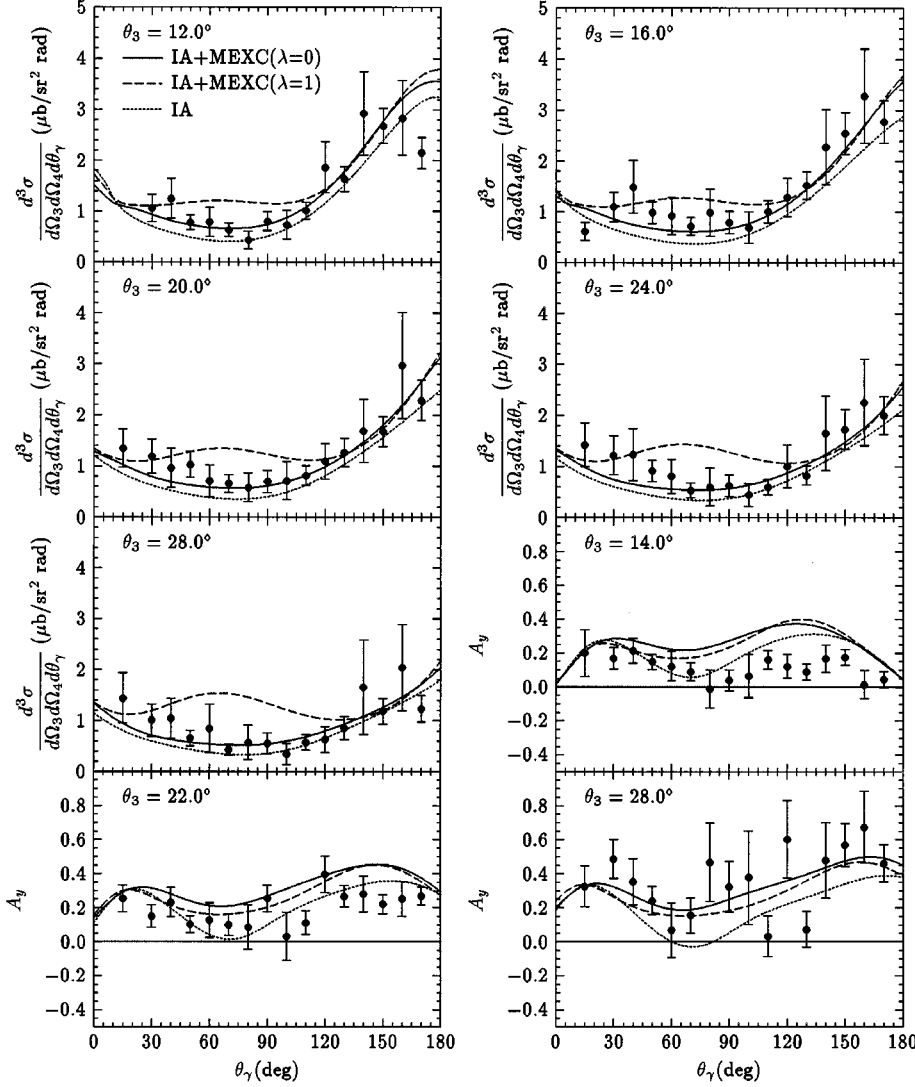


FIG. 15. Coplanar  $pp$ -bremsstrahlung data at  $E_{\text{lab}}=280$  MeV and  $\theta_4=12.4^\circ$  compared to RuhrPot calculations including (IA+MEXC) or excluding (IA) relativistic meson-exchange currents with pv ( $\lambda=0$ ) or ps ( $\lambda=1$ )  $NN\pi$  interactions. The exchange currents include wave function reorthonormalization and meson-recoil currents,  $NN\bar{N}$  pair creation and annihilation currents,  $\rho\pi\gamma + \omega\pi\gamma + \rho\eta\gamma + \omega\eta\gamma$  vector-meson decay currents and  $N\Delta\gamma(\pi,\rho,\Gamma_\Delta=115 \text{ MeV})$  exchange currents.

where  $\beta=\vec{\pi}$  or  $\vec{\rho}$  and the factor  $-g_{\sigma\tau}$  and all references to the Lorentz indices  $\sigma$  and  $\tau$  are to be ignored for the scalar mesons. The exact form of  $D^\beta$  is given in Appendix A, but here it is sufficient to note the nonrelativistic limit,

$$D_1^\beta \sim D_3^\beta \sim \frac{-1}{2\omega_\beta(\vec{q}_2)(m_\Delta - m + \omega_\beta)} \times \left[ 1 + \frac{(m_\Delta - m)^2}{\omega_\beta(\vec{q}_2)[m_\Delta - m + \omega_\beta(\vec{q}_2)]} \right] \quad (4.8)$$

The first term in the brackets of Eq (4.8) represents the  $N\Delta\gamma$  initial- and final-state strong-interaction amplitudes, and the second term gives the  $N\Delta\gamma$  wave function reorthonormalization and meson-recoil currents. Unlike their analogous  $NN\gamma$  terms, where only one-body currents survive in the static limit, the  $N\Delta\gamma$  wave function reorthonormalization and meson-recoil currents do *not* vanish in static limit—even for soft photons (cf. [20]). Indeed noting that  $m_\Delta - m \sim 2m_\pi$  shows that these contributions make an im-

portant contribution to the intermediate-state  $\Delta N$  amplitudes in the low-energy observables.

Since the coupled channel  $t$  matrices have been calculated only in the barycentric frame, it remains to either calculate their boost operators, or demonstrate that they are effectively Lorentz invariant. In Sec. IV A (see Fig. 9) we demonstrated such invariance for a toy-model boson-exchange potential and commented on the reliability of guessing minimal relativity factors. We anticipate that a similar approximate invariance will probably hold for the coupled channel  $NN \rightleftharpoons NN$   $t$  matrices involving intermediate  $\Delta N$  states. However, in Fig. 20 we observe that the corresponding  $N\Delta\gamma$  initial- and final-state interaction amplitudes calculated in the average barycentric frame of Eq. (3.33) are seriously different from the corresponding results evaluated in the  $I$  and  $F$  frames of Eqs. (3.38) and (3.40). This shows that the leading-order contributions to the coupled channel  $\Delta N \rightleftharpoons NN$  and  $NN \rightleftharpoons \Delta N$   $t$  matrices are poorly approximated under the assumption that they are Lorentz invariant.

We conclude that a nonperturbative description of the  $\Delta$  isobar amplitudes via coupled channel  $t$ -matrix calculations involves two complications.

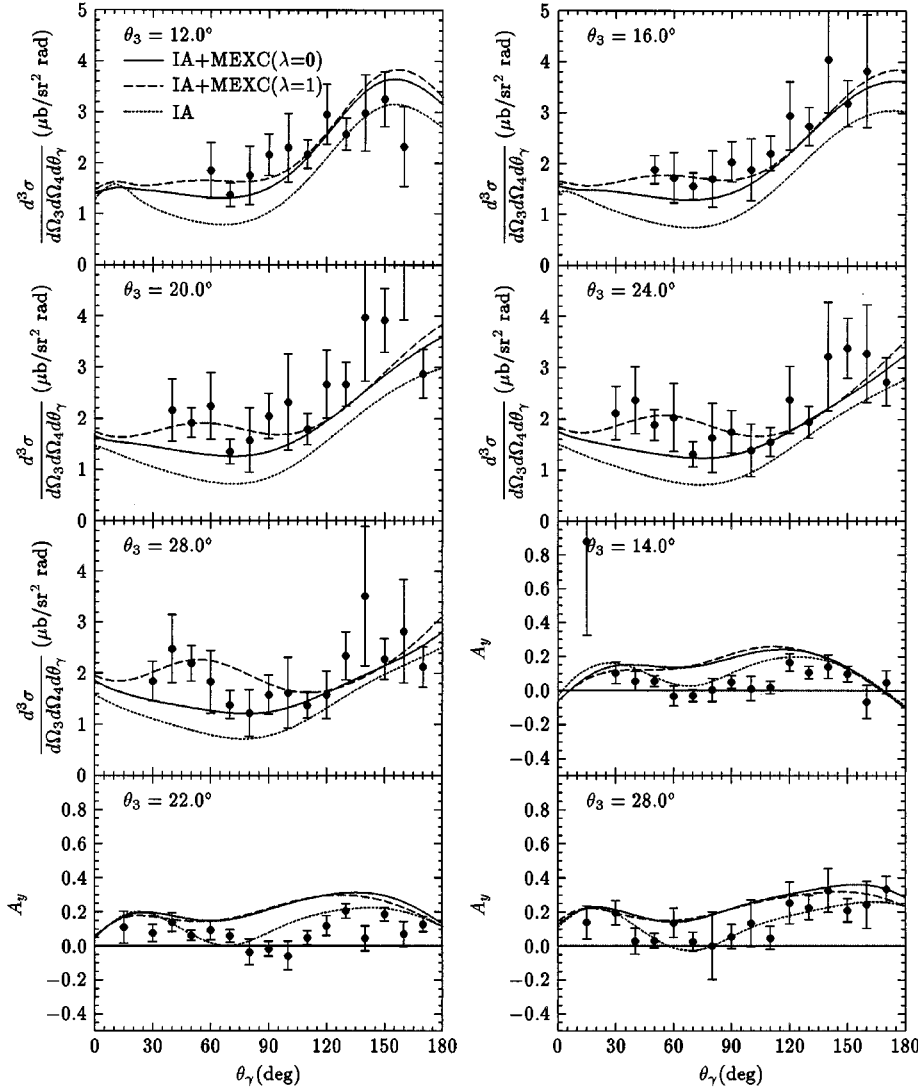


FIG. 16. Same as Fig. 15 except that  $\theta_4 = 17.3^\circ$ .

(1) There are nonvanishing contributions from the  $N\Delta\gamma$  wave function reorthonormalization and meson-recoil terms. The neglect of these two-body currents contributes serious errors at low energies.

(2) The initial- and final-state  $N\Delta\gamma$  interactions are poorly approximated in the absence of boost operators. The neglect of boost operators contributes serious errors at high energies.

As such, a meaningful specification of nonperturbative  $\Delta$  contributions requires the calculation of two-body currents and boost operators. This has not been recognized in the past. Although the first requirement can easily be satisfied by retaining a subset of the exchange currents we have presented in this work, there are outstanding problems that need to be solved if boost operators are to be defined beyond  $\mathcal{O}(1/m^4)$ . Such developments stand as a challenge for future theoretical work but can only be approached within a model providing a consistent and microscopic description of all meson-baryon dynamics.

### H. Relativistic effects

In earlier work [1] we presented selected  $pp$ -bremsstrahlung observables calculated using RuhrPot wave functions and the relativistic impulse current. The rescatter-

ing contributions of Fig. 1(c) were retained, as were the relativistic  $\rho\pi\gamma$ ,  $\omega\pi\gamma$ ,  $\rho\eta\gamma$ , and  $\omega\eta\gamma$  exchange currents. We also included the  $N\Delta\gamma$  currents with  $\pi$  and  $\rho$  exchange in the complete static limit, as defined in Sec. III B 5. No form of soft-photon approximation was adopted at any stage.

In the present work we have extended the exchange currents to include the wave function reorthonormalization and meson-recoil currents of Eq. (3.9) and the  $NN$ -pair creation and annihilation currents [for both  $(\lambda=0)$   $p\nu$  and  $(\lambda=1)$   $ps$   $NN\pi$  couplings] of Eq. (3.11) that are required for a truly relativistic description of the  $NN\gamma$  vertex. We have also replaced the complete static limit description of the dominant  $N\Delta\gamma(\pi)$  exchange current with the relativistic upgrade of Eq. (3.22).

In Fig. 21 we consider the magnitude of these purely relativistic effects by comparing with our earlier descriptions of the meson-exchange currents. We consider here only the  $p\nu$   $NN\pi$  coupling ( $\lambda=0$ ). From Figs 10, 12, and 13 we already know that the largest difference between these exchange current results stems from the relativistic corrections to the  $N\Delta\gamma(\pi)$  contribution. In addition, from Fig. 12 and Secs. III B 5 and IV D we note that this difference results from the neglect of the  $N-\Delta$  mass difference in the complete static

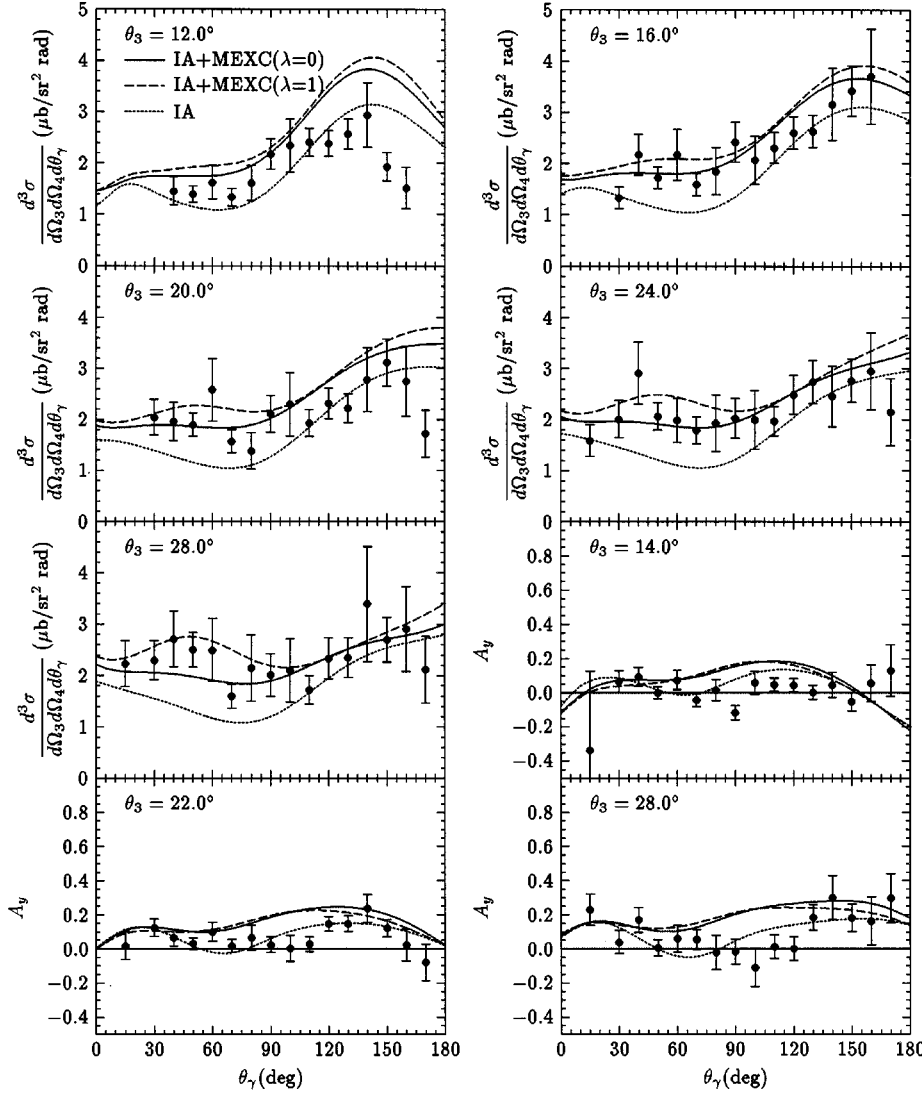


FIG. 17. Same as Fig. 15 except that  $\theta_4 = 21.2^\circ$ .

limit exchange current operators used in [1]. Although we find no need to change the qualitative conclusions reported in [1], a comparison of  $pp$ -bremsstrahlung calculations with experimental data near the  $\pi$ -production threshold clearly requires a relativistic description of the isovector meson-exchange currents.

## V. CONCLUSIONS

We have presented a parameter-free and relativistic extension of the RuhrPot meson-baryon model to define the dominant isoscalar meson-exchange currents. These include the first relativistic calculations for the wave function reorthonormalization, meson-recoil, and  $N\bar{N}$ -pair creation and annihilation currents in  $pp$ -bremsstrahlung. We also included the fully relativistic  $\rho\pi\gamma$ ,  $\omega\pi\gamma$ ,  $\rho\eta\gamma$ , and  $\omega\eta\gamma$  currents and a relativistic upgrade to our earlier  $N\Delta\gamma(\pi,\rho)$  exchange currents [1,15].

The results of these calculations show that the meson-exchange contributions to the  $pp$ -bremsstrahlung observables below the  $\pi$ -production threshold are large. As such, a meaningful interpretation of experiment obviously requires a completely consistent description of the meson-baryon dynamics defining the  $NN$  interaction, the exchange currents,

and the form factors that they contain.

Although the wave function renormalization and meson-recoil contributions are well known to cancel in the static limit for soft photons, this cancellation is poorly satisfied in bremsstrahlung experiments where the kinematics has been contrived to maximize the photon energy. As such, retaining these contributions is necessary if the orthonormality of the wave functions is to be preserved. Although these two-body currents have never before been included in bremsstrahlung calculations, they are necessary for a relativistic description of the  $NN\gamma$  vertex.

The motivation for developing such a relativistic scheme is found in one of the oldest outstanding puzzles in nuclear physics. The Lorentz structure of the  $NN\pi$  Lagrangian  $\mathcal{L}_{NN\pi}$  is universally accepted to comprise an unknown mixture of  $ps$  ( $\lambda=1$ ) and  $pv$  ( $\lambda=0$ ) couplings. This mixture cannot be distinguished by any nonrelativistic calculation and, for quite different reasons, makes almost no impact on relativistic calculations for the  $N\pi$  scattering lengths. However, within our relativistic framework we have shown that the existing  $pp$ -bremsstrahlung data indicate  $\lambda$  is small. This is surely the most reliable assessment of the  $NN\pi$  Lagrangian available to date.

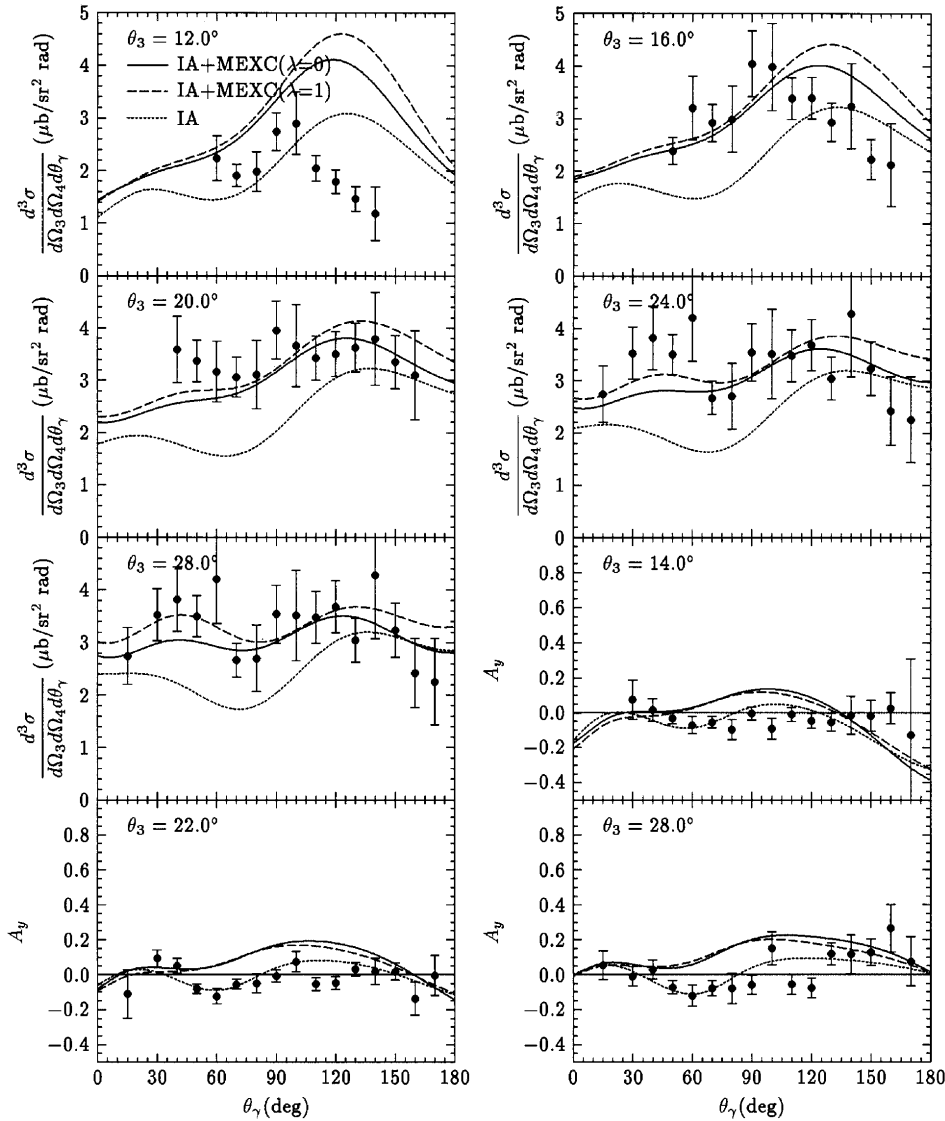


FIG. 18. Same as Fig. 15 except that  $\theta_4 = 27.8^\circ$ .

We quantified the  $VP\gamma$  exchange current contributions and noted their obvious relationship to the  $NN$  interaction. While the small vector-meson couplings in the RuhrPot  $NN$  interaction render these effects no larger than the  $NN$ -

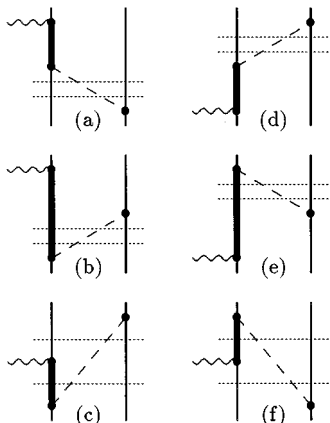


FIG. 19.  $N\Delta\gamma$  wave function reorthonormalization and meson-recoil exchange currents. These currents are necessary to preserve the orthonormality of the initial- and final-state wave functions described by  $NN$ ,  $\Delta N$  coupled channel transition  $t$  matrices.

interaction model differences in impulse approximation, we noted the necessity to include these currents in calculations for models using large  $NN\omega$  and  $NN\rho$  couplings (e.g., Bonn B). However, the largest isovector exchange current in  $pp$ -bremsstrahlung results from intermediate-state isobar excitation via  $\pi$  exchange. We investigated a series of approximations for this current and found that a relativistic description is necessary. Given the practical importance of this result, a compact closed form expression was provided and the sources of error in various approximations were identified.

We demonstrated our earlier assertion [1,15] that the  $N\Delta\gamma$  wave function reorthonormalization and meson-recoil contributions do *not* vanish, even in the static limit for soft photons. Their neglect in recent applications [19,20] indicates that the the orthonormality of the initial- and final-state wave functions is not preserved. In a perturbative analysis we showed that the assumed Lorentz invariance of the  $NN \Rightarrow NN$  interactions is accurate to about 3%, but that a similar assumption [19,20] for the  $NN \Rightarrow \Delta N$  interaction implies unacceptable errors of around 20%. We noted that a nonperturbative development of our parameter-free calculations requires inclusion of the  $N\Delta\gamma$  wave function reor-

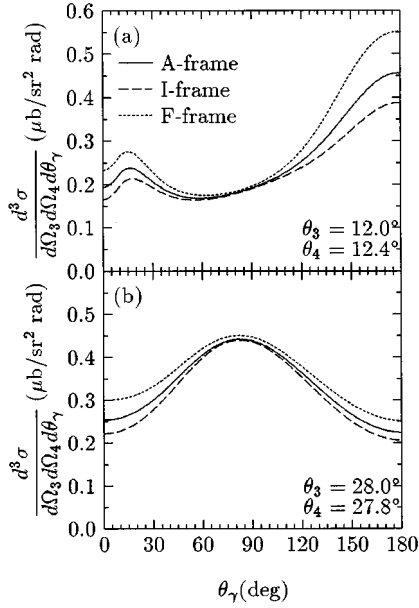


FIG. 20. Comparison of perturbative  $N\Delta$  initial- and final-state correlation amplitudes calculated in the (average barycentric) A frame and compared to corresponding results that are obtained in the initial- and final-state barycentric frames. The discrepancies show the need for boost operators and indicate errors of about 20% result when the  $NN \Rightarrow \Delta N$   $t$  matrix is assumed to be Lorentz invariant.

thonormalization and meson-recoil exchange currents (for which exact expressions were provided) and the application of boost operators. The need for more precise experimental data has been stressed.

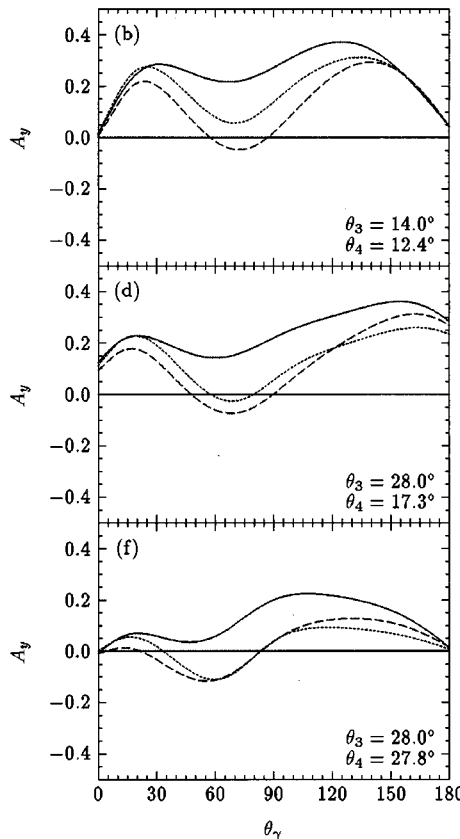
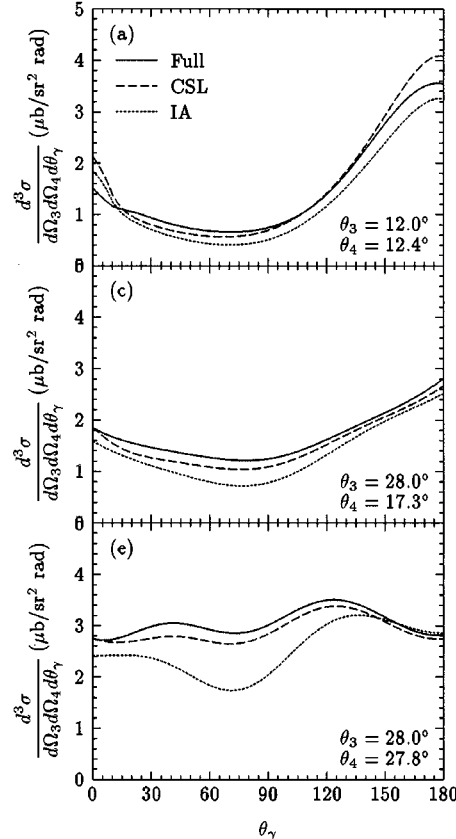


FIG. 21. Selected results from Figs. 15–18 using the  $ps NN\pi$  coupling with (full) and without (IA) the relativistic exchange currents, now compared with the (CSL) results of Ref. [1]. The CSL results differ from the full ones in that the wave function reorthonormalization, meson-recoil, and  $NN$ -pair currents are neglected entirely and the  $N\Delta\gamma(\pi)$  exchange current is taken in the complete static limit. The largest numerical difference in the meson-exchange current results can be traced to the neglect of the  $N-\Delta$  mass difference in the CSL operators. See also Secs. III B 5 and IV D for a detailed discussion.

## ACKNOWLEDGMENTS

This work is supported by COSY-KFA Jülich (41140512), the Deutsche Forschungsgemeinschaft (Ga 153/11-4), and BMFT.

## APPENDIX A: NONPERTURBATIVE $N\Delta\gamma$ AMPLITUDES

Within the formalism of Sec. II B, a nonperturbative description of the  $\Delta$ -isobar contributions requires our partition of the Hilbert space to be modified such that

$$\mathcal{H}_{\eta_1} = \{|NN\rangle\}, \quad \mathcal{H}_{\eta_2} = \{|\Delta N\rangle\}, \quad \mathcal{H}_{\eta_3} = \{|N\Delta\rangle\},$$

$$\mathcal{H}_{\eta_4} = \{|\Delta\Delta\rangle\}, \quad \mathcal{H}_{\lambda} = \{|\text{the rest}\rangle\} \quad (\text{A1})$$

with projection operators satisfying  $\eta = \sum_{i=1}^4 \eta_i$  and  $\eta_i \eta_j = \eta_i \delta_{ij}$ . Denoting an arbitrary operator causing transitions from the  $\eta_i$  space to the  $\eta_j$  space as  $\eta_j \mathcal{O} \eta_i = \mathcal{O}_{ji}$ , we require [in analogy to Eq. (2.22)] matrix elements of the form

$$[\mathcal{M}_{fi}]_{11} = N \vec{\epsilon}(\vec{k}, \lambda) \sum_{i,j=1}^4 \langle \vec{p}_3 \vec{p}_4; \alpha_j | \eta_1 [1 + t_{1i}^{(-)\dagger} G_{1i}] [\vec{J}_{\text{eff}}]_{ij} \times [1 + G_{j1} t_{j1}^{(+)}] \eta_1 | \vec{p}_1 \vec{p}_2; \alpha_i \rangle, \quad (\text{A2})$$

where we have denoted the effective one+two-body current density as



$$[\vec{J}_{\text{eff}}]_{ij} = \eta_i \left[ J + JA + A^\dagger J + A^\dagger JA - \frac{1}{2} JA^\dagger A - \frac{1}{2} A^\dagger AJ + \dots \right] \eta_j. \quad (\text{A3})$$

First consider the amplitudes involving an effective current describing  $NN \rightarrow NN$  transitions, which must therefore be

taken between initial- and final-state wave functions constructed from the  $NN \rightarrow NN$   $t$  matrix. These amplitudes include the dominant  $NN\gamma$  impulse currents, as well as contributions from the  $NN\gamma$  wave function reorthonormalization and meson-recoil currents. [Adopting (A1) does not alter the exact expressions for these currents given by Eqs. (3.9) and (3.10).] However, we now have additional contributions, as shown in Fig. 19, which are given by Eq. (4.7) with

$$D_1^\beta = \frac{1}{[E_3 - E_{\Delta 1k} - \omega_\beta(\vec{q}_2)][E_2 - E_4 - \omega_\beta(\vec{q}_2)]} - \frac{1}{2[E_4 - E_2 - \omega_\beta(\vec{q}_2)][E_1 - E_3 - \omega_\beta(\vec{q}_2)]} - \frac{1}{2[E_3 - E_{\Delta 1k} - \omega_\beta(\vec{q}_2)][E_1 + E_2 - E_{\Delta 1k} - E_4 - \omega_\beta(\vec{q}_2)]},$$

$$D_3^\beta = \frac{1}{[E_4 - E_2 - \omega_\beta(\vec{q}_2)][E_1 - E_{\Delta 3k} - \omega_\beta(\vec{q}_2)]} - \frac{1}{2[E_3 - E_1 - \omega_\beta(\vec{q}_2)][E_2 - E_4 - \omega_\beta(\vec{q}_2)]} - \frac{1}{2[E_3 + E_4 - E_{\Delta 3k} - E_2 - \omega_\beta(\vec{q}_2)][E_1 - E_{\Delta 3k} - \omega_\beta(\vec{q}_2)]}, \quad (\text{A4})$$

where  $\beta = \vec{\pi}$  or  $\vec{\rho}$ . Unlike their analogous  $NN\gamma$  terms, these  $N\Delta\gamma$  wave function reorthonormalization and meson-recoil currents do *not* vanish in the static limit. Their inclusion is required to preserve the orthonormality of the hadronic wave functions.

Next consider the amplitudes involving an effective current describing  $\Delta N \rightleftharpoons NN$  transitions, which must therefore be taken between initial- and final-state wave functions constructed from  $\Delta N \rightleftharpoons NN$  and  $NN \rightarrow NN$   $t$  matrices.

$$[\mathcal{M}_{fi}]_{11} = N\vec{\epsilon}(\vec{k}, \lambda) \langle \vec{p}_3 \vec{p}_4; \alpha_f | \eta_1 [1 + t_{11}^{(-)\dagger} G_{11}] [\vec{J}_{\text{eff}}]_{12} [G_{21} t_{21}^{(+)}] \eta_1 | \vec{p}_1 \vec{p}_2; \alpha_i \rangle + N\vec{\epsilon}(\vec{k}, \lambda) \langle \vec{p}_3 \vec{p}_4; \alpha_f | \eta_1 [t_{12}^{(-)\dagger} G_{12}] [\vec{J}_{\text{eff}}]_{21} [1 + G_{11} t_{11}^{(+)}] \eta_1 | \vec{p}_1 \vec{p}_2; \alpha_i \rangle + (1, 3 \rightleftharpoons 2, 3). \quad (\text{A5})$$

These are the  $N\Delta\gamma$  initial- and final-state interaction amplitudes and should obviously be specified in a consistent frame. However, the  $t$  matrices are available only in the barycentric frame, yet are required for the initial- and final-state interactions of Eq. (A5) in barycentric frames which differ by the photon momentum. The procedure adopted in recent works [19,20] is to attach (guessed) off-shell minimal relativity factors and assume this renders the initial- and final-state interaction terms individually Lorentz invariant. Rather than adopt this assumption, we provide an exact specification of the leading-order contributions to these amplitudes via Eq. (4.7) with

$$D_1^\beta = \frac{1}{2(E_3 + E_4 - E_{\Delta 1k} - E_2)} \times \left[ \frac{1}{E_3 - E_{\Delta 1k} - \omega_\beta} - \frac{1}{E_4 - E_2 - \omega_\beta} \right],$$

$$D_3^\beta = \frac{1}{2(E_1 + E_2 - E_{\Delta 3k} - E_4)} \times \left[ \frac{1}{E_1 - E_{\Delta 3k} - \omega_\beta} - \frac{1}{E_2 - E_4 - \omega_\beta} \right]. \quad (\text{A6})$$

## APPENDIX B: VERTEX FUNCTIONS

### 1. Interaction energies for strong vertices

For a meson with momentum  $\vec{q}$  and mass  $m_\beta$  we define

$$N_\beta = g_{NN\beta} \left\{ \frac{\mathcal{E}_i \mathcal{E}_f}{(2\pi)^3 8 \omega_\beta E_f E_i} \right\}^{1/2}, \quad \omega_\beta = \sqrt{(\vec{q})^2 + m_\beta^2}. \quad (\text{B1})$$

The interaction energies  $\langle 0 | b(\vec{p}_f) - \int d^3x \Gamma_{NN\beta} b^\dagger(\vec{p}_i) | 0 \rangle$  for the coupling of mesons to the positive-frequency nucleon current are

$$H_{NN\pi} = N_\pi h_{NN\pi} \vec{\tau}, \quad H_{NN\rho} = N_\rho \epsilon_{\mu\nu} h_{NN\rho}^\mu \vec{\tau},$$

$$H_{NN\delta} = N_\delta h_{NN\delta} \vec{\tau}, \quad (\text{B2a})$$

$$h_{NN\pi} = -i F_{NN\pi} \vec{\sigma} \cdot \left[ \frac{\vec{p}_f}{\mathcal{E}_f} - \frac{\vec{p}_i}{\mathcal{E}_i} \right], \quad (\text{B2b})$$

$$h_{NN\rho}^0 = \left[ F_{NN\rho}^{(1)} + \kappa_\rho F_{NN\rho}^{(2)} \left[ 1 - \frac{E_f + E_i}{2m} \right] \right] \\ + \left[ F_{NN\rho}^{(1)} + \kappa_\rho F_{NN\rho}^{(2)} \left[ 1 + \frac{E_f + E_i}{2m} \right] \right] \\ \times \left[ \frac{\vec{p}_f \cdot \vec{p}_i}{\mathcal{E}_f \mathcal{E}_i} + \frac{i\vec{\sigma} \cdot (\vec{p}_f \times \vec{p}_i)}{\mathcal{E}_f \mathcal{E}_i} \right], \quad (\text{B2c})$$

$$\vec{h}_{NN\rho} = [F_{NN\rho}^{(1)} + \kappa_\rho F_{NN\rho}^{(2)}] \left[ \frac{\vec{p}_f}{\mathcal{E}_f} + \frac{\vec{p}_i}{\mathcal{E}_i} + i\vec{\sigma} \times \left[ \frac{\vec{p}_f}{\mathcal{E}_f} - \frac{\vec{p}_i}{\mathcal{E}_i} \right] \right] \\ - \frac{\kappa_\rho F_{NN\rho}^{(2)}}{2m} (\vec{p}_f + \vec{p}_i) \left[ 1 - \frac{\vec{p}_f \cdot \vec{p}_i}{\mathcal{E}_f \mathcal{E}_i} - \frac{i\vec{\sigma} \cdot (\vec{p}_f \times \vec{p}_i)}{\mathcal{E}_f \mathcal{E}_i} \right], \quad (\text{B2d})$$

$$h_{NN\delta} = F_{NN\delta} \left[ 1 - \frac{\vec{p}_f \cdot \vec{p}_i}{\mathcal{E}_f \mathcal{E}_i} + \frac{i\vec{\sigma} \cdot (\vec{p}_f \times \vec{p}_i)}{\mathcal{E}_f \mathcal{E}_i} \right]. \quad (\text{B2e})$$

The interaction energies  $\langle 0|b(\vec{p}_f) - \int d^3x \Gamma_{NN\beta} d(-\vec{p}_i)|0\rangle$  for meson couplings to the pair-creation current are

$$H_{NN\pi} = N_\pi h_{NN\pi} \vec{\tau}, \quad H_{NN\rho} = N_\rho \epsilon_\mu h_{NN\rho}^\mu \vec{\tau}, \\ H_{NN\delta} = N_\delta h_{NN\delta} \vec{\tau}, \quad (\text{B3a})$$

$$h_{NN\pi} = +iF_{NN\pi} \left\{ \left[ 1 - (1-\lambda) \frac{E_i}{m} \right] + \left[ 1 + (1-\lambda) \frac{E_i}{m} \right] \right. \\ \left. \times \left[ \frac{\vec{p}_f \cdot \vec{p}_i}{\mathcal{E}_f \mathcal{E}_i} + i\vec{\sigma} \cdot \left( \frac{\vec{p}_f \times \vec{p}_i}{\mathcal{E}_f \mathcal{E}_i} \right) \right] \right\}, \quad (\text{B3b})$$

$$h_{NN\rho}^0 = \left[ F_{NN\rho}^{(1)} + \kappa_\rho F_{NN\rho}^{(2)} \left[ 1 + \frac{E_f - E_i}{2m} \right] \right] \frac{\vec{\sigma} \cdot \vec{p}_f}{\mathcal{E}_f} \\ - \left[ F_{NN\rho}^{(1)} + \kappa_\rho F_{NN\rho}^{(2)} \left[ 1 - \frac{E_f - E_i}{2m} \right] \right] \frac{\vec{\sigma} \cdot \vec{p}_i}{\mathcal{E}_i}, \quad (\text{B3c})$$

$$\vec{h}_{NN\rho} = \left[ F_{NN\rho}^{(1)} + \kappa_\rho F_{NN\rho}^{(2)} \left[ 1 - \frac{E_i}{m} \right] \right] \vec{\sigma} + \frac{\kappa_\rho F_{NN\rho}^{(2)}}{2m} (\vec{p}_f + \vec{p}_i) \\ \times \left[ \frac{\vec{\sigma} \cdot \vec{p}_f}{\mathcal{E}_f} + \frac{\vec{\sigma} \cdot \vec{p}_i}{\mathcal{E}_i} \right] + \left[ F_{NN\rho}^{(1)} + \kappa_\rho F_{NN\rho}^{(2)} \left[ 1 + \frac{E_i}{m} \right] \right] \\ \times \left[ \frac{i(\vec{p}_f \times \vec{p}_i)}{\mathcal{E}_f \mathcal{E}_i} + \frac{\vec{\sigma}(\vec{p}_f \cdot \vec{p}_i)}{\mathcal{E}_f \mathcal{E}_i} - \frac{\vec{p}_f(\vec{\sigma} \cdot \vec{p}_i)}{\mathcal{E}_f \mathcal{E}_i} - \frac{(\vec{\sigma} \cdot \vec{p}_f)\vec{p}_i}{\mathcal{E}_f \mathcal{E}_i} \right], \quad (\text{B3d})$$

$$h_{NN\delta} = -F_{NN\delta} \left[ \frac{\vec{\sigma} \cdot \vec{p}_f}{\mathcal{E}_f} + \frac{\vec{\sigma} \cdot \vec{p}_i}{\mathcal{E}_i} \right]. \quad (\text{B3e})$$

The interaction energies  $\langle 0|d^\dagger(-\vec{p}_f) - \int d^3x \Gamma_{NN\beta} b^\dagger(\vec{p}_i)|0\rangle$  for meson couplings to the pair-annihilation current are

$$H_{NN\pi} = N_\pi h_{NN\pi} \vec{\tau}, \quad H_{NN\rho} = N_\rho \epsilon_\mu h_{NN\rho}^\mu \vec{\tau}, \\ H_{NN\delta} = N_\delta h_{NN\delta} \vec{\tau} \quad (\text{B4a})$$

$$h_{NN\pi} = -iF_{NN\pi} \left\{ \left[ 1 - (1-\lambda) \frac{E_f}{m} \right] + \left[ 1 + (1-\lambda) \frac{E_f}{m} \right] \right. \\ \left. \times \left[ \frac{\vec{p}_f \cdot \vec{p}_i}{\mathcal{E}_f \mathcal{E}_i} + i\vec{\sigma} \cdot \left( \frac{\vec{p}_f \times \vec{p}_i}{\mathcal{E}_f \mathcal{E}_i} \right) \right] \right\}, \quad (\text{B4b})$$

$$h_{NN\rho}^0 = \left[ F_{NN\rho}^{(1)} + \kappa_\rho F_{NN\rho}^{(2)} \left[ 1 - \frac{E_f - E_i}{2m} \right] \right] \frac{\vec{\sigma} \cdot \vec{p}_i}{\mathcal{E}_i} \\ - \left[ F_{NN\rho}^{(1)} + \kappa_\rho F_{NN\rho}^{(2)} \left[ 1 + \frac{E_f - E_i}{2m} \right] \right] \frac{\vec{\sigma} \cdot \vec{p}_f}{\mathcal{E}_f}, \quad (\text{B4c})$$

$$\vec{h}_{NN\rho} = \left[ F_{NN\rho}^{(1)} + \kappa_\rho F_{NN\rho}^{(2)} \left[ 1 - \frac{E_f}{m} \right] \right] \vec{\sigma} + \frac{\kappa_\rho F_{NN\rho}^{(2)}}{2m} (\vec{p}_f + \vec{p}_i) \\ \times \left[ \frac{\vec{\sigma} \cdot \vec{p}_f}{\mathcal{E}_f} + \frac{\vec{\sigma} \cdot \vec{p}_i}{\mathcal{E}_i} \right] + \left[ F_{NN\rho}^{(1)} + \kappa_\rho F_{NN\rho}^{(2)} \left[ 1 + \frac{E_f}{m} \right] \right] \\ \times \left[ \frac{i(\vec{p}_f \times \vec{p}_i)}{\mathcal{E}_f \mathcal{E}_i} + \frac{\vec{\sigma}(\vec{p}_f \cdot \vec{p}_i)}{\mathcal{E}_f \mathcal{E}_i} - \frac{\vec{p}_f(\vec{\sigma} \cdot \vec{p}_i)}{\mathcal{E}_f \mathcal{E}_i} - \frac{(\vec{\sigma} \cdot \vec{p}_f)\vec{p}_i}{\mathcal{E}_f \mathcal{E}_i} \right], \quad (\text{B4d})$$

$$h_{NN\delta} = -F_{NN\delta} \left[ \frac{\vec{\sigma} \cdot \vec{p}_f}{\mathcal{E}_f} + \frac{\vec{\sigma} \cdot \vec{p}_i}{\mathcal{E}_i} \right], \quad (\text{B4e})$$

where all strong form factors are evaluated at  $Q^2 = -q^2 = -(E_f - E_i)^2 + \vec{q}^2$ .

For the  $N\Delta\beta$  vertices we define [see Eq. (3.7)]

$$N_\pi^\Delta = \frac{ig_{N\Delta\pi} F_{N\Delta\pi}}{2m} \left[ \frac{\mathcal{E}_\Delta \mathcal{E}}{(2\pi)^3 8 \omega_\pi E_\Delta E} \right]^{1/2}, \\ N_\rho^\Delta = \frac{g_{NN\rho} G_M^{N\Delta\rho}}{2m} \frac{g_{\Delta N\pi}}{g_{NN\pi}} \left[ \frac{\mathcal{E}_\Delta \mathcal{E}}{(2\pi)^3 8 \omega_\rho E_\Delta E} \right]^{1/2}. \quad (\text{B5})$$

The interaction energies  $\langle 0|b_\Delta(\vec{p}) - \int d^3x \Gamma_{\Delta N\beta} b^\dagger(\vec{p})|0\rangle$  for meson couplings to the  $N \rightarrow \Delta$  current are

$$H_{\Delta N\pi} = N_\pi^\Delta h_{\Delta N\pi} \vec{\tau}_{N\Delta}, \quad H_{\Delta N\rho} = N_\rho^\Delta h_{\Delta N\rho}^\nu \epsilon_\nu \vec{\tau}_{N\Delta}, \quad (\text{B6a})$$

$$h_{\Delta N\pi} = -\vec{\sigma}_{N\Delta} \cdot \left[ \vec{p}_\Delta \left( \frac{E}{m_\Delta} - \frac{(\vec{p}_\Delta \cdot \vec{p})}{\mathcal{E}_\Delta m_\Delta} \right) - \vec{p} \right] \\ \times \left[ 1 - \left( \frac{\vec{\sigma} \cdot \vec{p}_\Delta}{\mathcal{E}_\Delta} \right) \left( \frac{\vec{\sigma} \cdot \vec{p}}{\mathcal{E}} \right) \right], \quad (\text{B6b})$$

$$\begin{aligned}
h_{\Delta N\rho} = & + \left[ \frac{-\vec{p}_\Delta \cdot \vec{\sigma}_{N\Delta}}{m_\Delta}; \vec{\sigma}_{N\Delta} + \vec{p}_\Delta \frac{\vec{\sigma}_{N\Delta} \cdot \vec{p}_\Delta}{\mathcal{E}_\Delta m_\Delta} \right]^\mu \left[ \left( \frac{\vec{\sigma} \cdot \vec{p}_\Delta}{\mathcal{E}_\Delta} \right) \right. \\
& + \left. \left( \frac{\vec{\sigma} \cdot \vec{p}}{\mathcal{E}} \right); \vec{\sigma} + \frac{(\vec{\sigma} \cdot \vec{p}_\Delta) \vec{\sigma} (\vec{\sigma} \cdot \vec{p})}{\mathcal{E}_\Delta \mathcal{E}} \right]^\lambda \\
& \times [(p_\Delta - p)_\mu \delta_\lambda^\nu - (p_\Delta - p)_\lambda \delta_\mu^\nu]. \quad (\text{B6c})
\end{aligned}$$

The interaction energies  $\langle 0 | b(\vec{p}) - f d^3 x \Gamma_{\Delta N \beta} b_\Delta^\dagger(\vec{p}_\Delta) | 0 \rangle$  for meson couplings to the  $\Delta \rightarrow N$  current are

$$H_{N\Delta\pi} = N_\pi^\Delta h_{N\Delta\pi} \vec{\tau}_{N\Delta}^\dagger, \quad H_{N\Delta\rho} = N_\rho^\Delta h_{N\Delta\rho}^\nu \epsilon_\nu \vec{\tau}_{N\Delta}^\dagger, \quad (\text{B7a})$$

$$\begin{aligned}
h_{N\Delta\pi} = & + \left[ 1 - \left( \frac{\vec{\sigma} \cdot \vec{p}_\Delta}{\mathcal{E}_\Delta} \right) \left( \frac{\vec{\sigma} \cdot \vec{p}}{\mathcal{E}} \right) \right] \vec{\sigma}_{N\Delta}^\dagger \\
& \times \left[ \vec{p}_\Delta \left( \frac{E}{m_\Delta} - \frac{\vec{p}_\Delta \cdot \vec{p}}{\mathcal{E}_\Delta m_\Delta} \right) - \vec{p} \right], \quad (\text{B7b})
\end{aligned}$$

$$\begin{aligned}
h_{N\Delta\rho}^\nu = & - \left[ \left( \frac{\vec{\sigma} \cdot \vec{p}_\Delta}{\mathcal{E}_\Delta} \right) + \left( \frac{\vec{\sigma} \cdot \vec{p}}{\mathcal{E}} \right); \vec{\sigma} + \frac{(\vec{\sigma} \cdot \vec{p}_\Delta) \vec{\sigma} (\vec{\sigma} \cdot \vec{p})}{\mathcal{E}_\Delta \mathcal{E}} \right]^\lambda \\
& \times \left[ \frac{-\vec{\sigma}_{N\Delta}^\dagger \cdot \vec{p}_\Delta}{m_\Delta}; \vec{\sigma}_{N\Delta}^\dagger + \vec{p}_\Delta \frac{(\vec{\sigma}_{N\Delta}^\dagger \cdot \vec{p}_\Delta)}{\mathcal{E}_\Delta m_\Delta} \right]^\mu \\
& \times [(p - p_\Delta)_\mu \delta_\lambda^\nu - (p - p_\Delta)_\lambda \delta_\mu^\nu]. \quad (\text{B7c})
\end{aligned}$$

## 2. Currents for electromagnetic vertices

We define

$$N_\gamma = \frac{e_p}{(2\pi)^3} \left\{ \frac{\mathcal{E}_i \mathcal{E}_f}{4E_f E_i} \right\}^{1/2}. \quad (\text{B8})$$

The photon coupling to the positive frequency nucleon current  $\langle 0 | b(\vec{p}_f) J_{\text{eff}}(0) b^\dagger(\vec{p}_i) | 0 \rangle$  is given by

$$J_{NN\gamma}^\mu = N_\gamma j_{NN\gamma}^\mu, \quad (\text{B9a})$$

$$\begin{aligned}
j_{NN\gamma}^0 = & \left[ F_{NN\gamma}^{(1)} + \kappa F_{NN\gamma}^{(2)} \left[ 1 - \frac{E_f + E_i}{2m} \right] \right] \\
& + \left[ F_{NN\gamma}^{(1)} + \kappa F_{NN\gamma}^{(2)} \left[ 1 + \frac{E_f + E_i}{2m} \right] \right] \\
& \times \left[ \frac{\vec{p}_f \cdot \vec{p}_i}{\mathcal{E}_f \mathcal{E}_i} + \frac{i\vec{\sigma} \cdot (\vec{p}_f \times \vec{p}_i)}{\mathcal{E}_f \mathcal{E}_i} \right], \quad (\text{B9b})
\end{aligned}$$

$$\begin{aligned}
\vec{j}_{NN\gamma} = & [F_{NN\gamma}^{(1)} + \kappa F_{NN\gamma}^{(2)}] \left[ \frac{\vec{p}_f}{\mathcal{E}_f} + \frac{\vec{p}_i}{\mathcal{E}_i} + i\vec{\sigma} \times \left[ \frac{\vec{p}_f}{\mathcal{E}_f} - \frac{\vec{p}_i}{\mathcal{E}_i} \right] \right] \\
& - \frac{\kappa F_{NN\gamma}^{(2)}}{2m} (\vec{p}_f + \vec{p}_i) \left[ 1 - \frac{\vec{p}_f \cdot \vec{p}_i}{\mathcal{E}_f \mathcal{E}_i} - \frac{i\vec{\sigma} \cdot (\vec{p}_f \times \vec{p}_i)}{\mathcal{E}_f \mathcal{E}_i} \right]. \quad (\text{B9c})
\end{aligned}$$

The photon coupling to the pair-creation current  $\langle 0 | b(\vec{p}_f) J_{\text{eff}}(0) d(-\vec{p}_i) | 0 \rangle$  is given by

$$J_{\bar{N}\bar{N}\gamma} = N_\gamma \epsilon_\mu j_{\bar{N}\bar{N}\gamma}^\mu, \quad (\text{B10a})$$

$$\begin{aligned}
j_{\bar{N}\bar{N}\gamma}^0 = & \left[ F_{NN\gamma}^{(1)} + \kappa F_{NN\gamma}^{(2)} \left[ 1 + \frac{E_f - E_i}{2m} \right] \right] \frac{\vec{\sigma} \cdot \vec{p}_f}{\mathcal{E}_f} \\
& - \left[ F_{NN\gamma}^{(1)} + \kappa F_{NN\gamma}^{(2)} \left[ 1 - \frac{E_f - E_i}{2m} \right] \right] \frac{\vec{\sigma} \cdot \vec{p}_i}{\mathcal{E}_i}, \quad (\text{B10b})
\end{aligned}$$

$$\begin{aligned}
\vec{j}_{\bar{N}\bar{N}\gamma} = & \left[ F_{NN\gamma}^{(1)} + \kappa F_{NN\gamma}^{(2)} \left[ 1 - \frac{E_i}{m} \right] \right] \vec{\sigma} + \frac{\kappa F_{NN\gamma}^{(2)}}{2m} (\vec{p}_f + \vec{p}_i) \\
& \times \left[ \frac{\vec{\sigma} \cdot \vec{p}_f}{\mathcal{E}_f} + \frac{\vec{\sigma} \cdot \vec{p}_i}{\mathcal{E}_i} \right] + \left[ F_{NN\gamma}^{(1)} + \kappa F_{NN\gamma}^{(2)} \left[ 1 + \frac{E_i}{m} \right] \right] \\
& \times \left[ \frac{i(\vec{p}_f \times \vec{p}_i)}{\mathcal{E}_f \mathcal{E}_i} + \frac{\vec{\sigma}(\vec{p}_f \cdot \vec{p}_i)}{\mathcal{E}_f \mathcal{E}_i} - \frac{\vec{p}_f(\vec{\sigma} \cdot \vec{p}_i)}{\mathcal{E}_f \mathcal{E}_i} - \frac{(\vec{\sigma} \cdot \vec{p}_f)\vec{p}_i}{\mathcal{E}_f \mathcal{E}_i} \right]. \quad (\text{B10c})
\end{aligned}$$

The photon coupling to the pair-annihilation current  $\langle 0 | d^\dagger(-\vec{p}_f) J_{\text{eff}}(0) b^\dagger(\vec{p}_i) | 0 \rangle$  is given by

$$J_{N\bar{N}\gamma} = N_\gamma \epsilon_\mu j_{N\bar{N}\gamma}^\mu, \quad (\text{B11a})$$

$$\begin{aligned}
j_{N\bar{N}\gamma}^0 = & \left[ F_{NN\gamma}^{(1)} + \kappa F_{NN\gamma}^{(2)} \left[ 1 - \frac{E_f - E_i}{2m} \right] \right] \frac{\vec{\sigma} \cdot \vec{p}_i}{\mathcal{E}_i} \\
& - \left[ F_{NN\gamma}^{(1)} + \kappa F_{NN\gamma}^{(2)} \left[ 1 + \frac{E_f - E_i}{2m} \right] \right] \frac{\vec{\sigma} \cdot \vec{p}_f}{\mathcal{E}_f}, \quad (\text{B11b})
\end{aligned}$$

$$\begin{aligned}
\vec{j}_{N\bar{N}\gamma} = & \left[ F_{NN\gamma}^{(1)} + \kappa F_{NN\gamma}^{(2)} \left[ 1 - \frac{E_f}{m} \right] \right] \vec{\sigma} + \frac{\kappa F_{NN\gamma}^{(2)}}{2m} (\vec{p}_f + \vec{p}_i) \\
& \times \left[ \frac{\vec{\sigma} \cdot \vec{p}_f}{\mathcal{E}_f} + \frac{\vec{\sigma} \cdot \vec{p}_i}{\mathcal{E}_i} \right] + \left[ F_{NN\gamma}^{(1)} + \kappa F_{NN\gamma}^{(2)} \left[ 1 + \frac{E_f}{m} \right] \right] \\
& \times \left[ \frac{i(\vec{p}_f \times \vec{p}_i)}{\mathcal{E}_f \mathcal{E}_i} + \frac{\vec{\sigma}(\vec{p}_f \cdot \vec{p}_i)}{\mathcal{E}_f \mathcal{E}_i} - \frac{\vec{p}_f(\vec{\sigma} \cdot \vec{p}_i)}{\mathcal{E}_f \mathcal{E}_i} - \frac{(\vec{\sigma} \cdot \vec{p}_f)\vec{p}_i}{\mathcal{E}_f \mathcal{E}_i} \right], \quad (\text{B11c})
\end{aligned}$$

where the electromagnetic form factors are defined as

$$\begin{aligned}
F_{NN\gamma}^{(1)} = & \frac{1}{2} F_{NN\gamma}^{(1);is} + \frac{1}{2} F_{NN\gamma}^{(1);iv} \tau^0, \\
\kappa_N F_{NN\gamma}^{(2)} = & \frac{1}{2} \kappa^{is} F_{NN\gamma}^{(2);iv} + \frac{1}{2} \kappa^{iv} F_{NN\gamma}^{(2);iv} \tau^0, \quad (\text{B12a})
\end{aligned}$$

$$\begin{aligned}
\Rightarrow \text{protons: } & F_{NN\gamma}^{(1)}(k^2=0) + \kappa_N F_{NN\gamma}^{(2)}(k^2=0) \\
= & (1) + \left( \frac{\kappa^{is} + \kappa^{iv}}{2} \right) = \mu_p,
\end{aligned}$$

$$(\text{B12b})$$

$$\begin{aligned}
\Rightarrow \text{neutrons: } & F_{NN\gamma}^{(1)}(k^2=0) + \kappa_N F_{NN\gamma}^{(2)}(k^2=0) \\
= & (0) + \left( \frac{\kappa^{is} - \kappa^{iv}}{2} \right) = \mu_n.
\end{aligned}$$

$$(\text{B12c})$$

For the  $N\Delta\gamma$  vertices we define [see Eq. (3.7)],

$$N_\gamma^\Delta = \frac{e_p}{(2\pi)^3 2m} \frac{G_M^{\text{iv}}}{2} \frac{g_{\Delta N\pi}}{g_{NN\pi}} \left[ \frac{\mathcal{E}_\Delta \mathcal{E}}{4E_\Delta E} \right]^{1/2};$$

$$G_M^{\text{iv}}(0) = 1 + \kappa^{\text{iv}} = 4.706. \quad (\text{B13})$$

The photon coupling to the  $N \rightarrow \Delta$  current  $\langle 0 | b_\Delta(\vec{p}) J_{\text{eff}}(0) b^\dagger(\vec{p}) | 0 \rangle$  is given by

$$J_{\Delta N\gamma} = N_\gamma^\Delta j_{\Delta N\gamma}^\nu \epsilon_\nu(\tau_{N\Delta})^0, \quad (\text{B14a})$$

$$j_{\Delta N\gamma}^\nu = + \left[ \frac{-\vec{\sigma}_{N\Delta} \cdot \vec{p}_\Delta}{m_\Delta}; \vec{\sigma}_{N\Delta} + \vec{p}_\Delta \frac{\vec{\sigma}_{N\Delta} \cdot \vec{p}_\Delta}{\mathcal{E}_\Delta m_\Delta} \right]^\mu$$

$$\times \left[ \left( \frac{\vec{\sigma} \cdot \vec{p}_\Delta}{\mathcal{E}_\Delta} \right) + \left( \frac{\vec{\sigma} \cdot \vec{p}}{\mathcal{E}} \right); \vec{\sigma} + \frac{(\vec{\sigma} \cdot \vec{p}_\Delta) \vec{\sigma} (\vec{\sigma} \cdot \vec{p})}{\mathcal{E}_\Delta \mathcal{E}} \right]^\lambda$$

$$\times [(p_\Delta - p)_\mu \delta_\lambda^\nu - (p_\Delta - p)_\lambda \delta_\mu^\nu]. \quad (\text{B14b})$$

The photon coupling to the  $\Delta \rightarrow N$  current  $\langle 0 | b(\vec{p}) J_{\text{eff}}(0) b_\Delta^\dagger(\vec{p}_\Delta) | 0 \rangle$  is given by

$$J_{N\Delta\gamma} = N_\gamma^\Delta j_{N\Delta\gamma}^\nu \epsilon_\nu(\tau_{N\Delta}^\dagger)^0, \quad (\text{B15a})$$

$$j_{N\Delta\gamma}^\nu = - \left[ \left( \frac{\vec{\sigma} \cdot \vec{p}_\Delta}{\mathcal{E}_\Delta} \right) + \left( \frac{\vec{\sigma} \cdot \vec{p}}{\mathcal{E}} \right); \vec{\sigma} + \frac{(\vec{\sigma} \cdot \vec{p}_\Delta) \vec{\sigma} (\vec{\sigma} \cdot \vec{p})}{\mathcal{E}_\Delta \mathcal{E}} \right]^\lambda$$

$$\times \left[ \frac{-\vec{p}_\Delta \cdot \vec{\sigma}_{N\Delta}^\dagger}{m_\Delta}; \vec{\sigma}_{N\Delta}^\dagger + \vec{p}_\Delta \frac{\vec{\sigma}_{N\Delta}^\dagger \cdot \vec{p}_\Delta}{\mathcal{E}_\Delta m_\Delta} \right]^\mu$$

$$\times [(p - p_\Delta)_\mu \delta_\lambda^\nu - (p - p_\Delta)_\lambda \delta_\mu^\nu]. \quad (\text{B15b})$$

The photon coupling to the vector-meson-decay current is given by

$$J_{VP\gamma}^\mu(q_P, q_V) = \frac{-e_p g_{VP\gamma} F_{VP\gamma}}{m_V} \frac{1}{(2\pi)^3}$$

$$\times \frac{1}{\sqrt{4\omega_V \omega_P}} \epsilon^{\mu\xi ab} \epsilon_\xi(\vec{q}_V, \lambda_V)$$

$$\times (q_P)_a (q_V)_b \quad (\text{B16})$$

where  $F_{VP\gamma}(k^2=0)=1$ ,  $q_V$  and  $q_P$  are the four-momenta delivered to the nucleons by the vector and pseudoscalar mesons, respectively.

### APPENDIX C: THE MOMENTUM-SPACE $NN\gamma$ RESCATTERING CALCULATION

The  $NN\gamma$  rescattering amplitudes in bremsstrahlung were first calculated by Brown [21] in  $r$  space. For  $p$ -space calculations, a recipe has already been given in [10], although the residue terms are valid only for soft photons and the dominant final-state interaction is scaled by (guessed) off-shell minimal relativity factors and cast into the  $I$  frame with a barycentric momentum  $k$ . This choice of frame does not minimize the effect of the neglected boost operators and the inclusion of minimal relativity factors disturbs the convergence properties of the  $p$  space integral.

Casting the entire rescattering amplitude into the  $A$  frame of Eq. (3.33) requires a somewhat different numerical procedure. We start from Eq. (3.44) and simplify our notation by defining

$$\mathcal{M}_{fi}^R = K \int \int H(\hat{p}) d\theta d\phi, \quad H(\hat{p}) = \int \frac{F(\vec{p})}{G_i(\vec{p}) G_f(\vec{p})} dp, \quad (\text{C1})$$

with

$$F(\vec{p}) = p^2 \sin\theta [E(\vec{p}_3 + \frac{1}{4}\vec{k}) + E(\vec{p} + \frac{1}{4}\vec{k})] [E(\vec{p}_1 - \frac{1}{4}\vec{k}) + E(\vec{p} - \frac{1}{4}\vec{k})]$$

$$\times \sum_{M_S M_S'} \langle \vec{p}_3 + \frac{1}{4}\vec{k}; S_f M_{S_f}; T_f M_T | [1 + i\chi \left( -\frac{\vec{k}}{2} \right)] t^{(-)\dagger} [1 - i\chi \left( -\frac{\vec{k}}{2} \right)] | \vec{p} + \frac{1}{4}\vec{k}; S_f M_S'; T_f M_T \rangle$$

$$\times \langle S_f M_S'; T_f M_T | J_{NN\gamma}[1] \left( -\vec{p} + \frac{\vec{k}}{2}, -\vec{p} - \frac{\vec{k}}{2} \right) | S_i M_S; T_i M_T \rangle$$

$$\times \langle \vec{p} - \frac{1}{4}\vec{k}; S_i M_S; T_i M_T | [1 + i\chi \left( +\frac{\vec{k}}{2} \right)] G_i t^{(+)} [1 - i\chi \left( +\frac{\vec{k}}{2} \right)] | \vec{p}_1 - \frac{1}{4}\vec{k}; S_i M_S; T_i M_T \rangle,$$

$$G_i(\vec{p}) = (\vec{p}_1 - \frac{1}{4}\vec{k})^2 - (\vec{p} - \frac{1}{4}\vec{k})^2 + i\eta_i = \Delta_i^2 - (p - \frac{1}{4}|\vec{k}|\cos\vartheta)^2 + i\eta_i,$$

$$G_f(\vec{p}) = (\vec{p}_3 + \frac{1}{4}\vec{k})^2 - (\vec{p} + \frac{1}{4}\vec{k})^2 + i\eta_f = \Delta_f^2 - (p + \frac{1}{4}|\vec{k}|\cos\vartheta)^2 + i\eta_f,$$

$$\Delta_i^2 = (\frac{1}{4}|\vec{k}|\cos\vartheta)^2 - \vec{p}_1 \cdot \vec{p}_2, \quad \Delta_f^2 = (\frac{1}{4}|\vec{k}|\cos\vartheta)^2 - \vec{p}_3 \cdot \vec{p}_4,$$

$$K = \frac{N}{2} (-1)^{(S_f + S_i + T_f + T_i)}, \quad (\text{C2})$$

with  $\cos\vartheta = \hat{p} \cdot \hat{k} = \sin\theta_p \sin\theta_k \cos(\phi_p - \phi_k) + \cos\theta_p \cos\theta_k$ . Within the (maximally symmetric)  $A$  frame the effects of the boost operators  $\chi(+\vec{k}/2)$  and  $\chi(-\vec{k}/2)$  can be expected to substantially cancel and will therefore be neglected in the present numerical applications. Their inclusion would change nothing that we will discuss in this appendix.

For  $\Delta_i, \Delta_f < 0$ , there are no poles on the real axis, but it is easy to see that there are singularities in the Green's functions at  $\vec{p} = \vec{p}_1, \vec{p}_2, \vec{p}_3, \vec{p}_4$  as well as  $(\vec{p}_1 - \vec{p}) \cdot (\vec{p}_2 - \vec{p})$  and  $(\vec{p}_3 - \vec{p}) \cdot (\vec{p}_4 - \vec{p})$ , the latter two requiring particular attention when  $\cos\vartheta_i = \pm 4\sqrt{\vec{p}_1 \cdot \vec{p}_2}/|\vec{k}|$  or  $\cos\vartheta_f = \pm 4\sqrt{\vec{p}_3 \cdot \vec{p}_4}/|\vec{k}|$  cause  $\Delta_i = 0$  or  $\Delta_f = 0$ , so that  $G_i^{-1}$  and/or  $G_f^{-1}$  each have a second-order pole (on the real axis). We adopt the utilitarian attitude of noting that for experiments below the  $\pi$ -production threshold, the second-order poles only occur at  $\theta_1^{\text{lab}}, \theta_2^{\text{lab}} < 6^\circ$ , and even then, only for  $\theta_\gamma^{\text{lab}} < 1^\circ$ . Since no data exist in this region, we simply defer a treatment of second order singularities and confine our attention to the kinematics containing the simple and separable poles,

$$p = p_i^{(\pm)} = + \frac{1}{4} |\vec{k}| \cos\vartheta \pm \Delta_i$$

$$\text{if } \Delta_i^2 \geq 0 \text{ then } \Delta_i = \left| p_i^{(\pm)} - \frac{1}{4} |\vec{k}| \cos\vartheta \right|,$$

$$p = p_f^{(\pm)} = - \frac{1}{4} |\vec{k}| \cos\vartheta \pm \Delta_f$$

$$\text{if } \Delta_f^2 \geq 0 \text{ then } \Delta_f = \left| p_f^{(\pm)} + \frac{1}{4} |\vec{k}| \cos\vartheta \right|, \quad (\text{C3})$$

and evaluate  $\Delta_i^2$  and  $\Delta_f^2$  to determine if poles exist on the positive real  $p$  axis. Defining such poles to be vectors so that  $\hat{p}_i^\pm = \hat{p}_f^\pm = \hat{p}$ , we obtain

$$H(\hat{p}) = V \cdot P \cdot \int dp \frac{F(\vec{p})}{\left[ \Delta_i^2 - \left( p - \frac{1}{4} |\vec{k}| \cos\vartheta \right)^2 \right] \left[ \Delta_f^2 - \left( p + \frac{1}{4} |\vec{k}| \cos\vartheta \right)^2 \right]} - Z, \quad (\text{C4})$$

where

$$Z = \frac{i\pi F(\vec{p}_i^{(+)})}{2\Delta_i G_f(p_i^{(+)})} + \frac{i\pi F(\vec{p}_i^{(-)})}{2\Delta_i G_f(p_i^{(-)})} + \frac{i\pi F(\vec{p}_f^{(+)})}{2\Delta_f G_i(p_f^{(+)})} + \frac{i\pi F(\vec{p}_f^{(-)})}{2\Delta_f G_i(p_f^{(-)})} \quad (\text{C5})$$

remains well defined. This formally completes the specification of the integral. However, for practical purposes, we need to add special forms of zero to smooth the divergences near the poles. With a simple generalization of

$$VP \int_{a_1}^{a_2} \frac{1}{k^2 - p^2} dp = \frac{1}{2k} \ln \left| \frac{a_2 + k}{a_2 - k} \frac{k - a_1}{k + a_1} \right| \quad (\text{C6})$$

we obtain

$$H = H_{p_i^{(+)}} + H_{p_i^{(-)}} + H_{p_f^{(+)}} + H_{p_f^{(-)}}, \quad (\text{C7})$$

where

$$H_{p_i^{(+)}} = \int_{a_1}^{a_2} \frac{1}{G_i(\vec{p})} \left[ \frac{F(\vec{p})}{G_f(\vec{p})} - \frac{F(\vec{p}_i^{(+)})}{G_f(\vec{p}_i^{(+)})} \right] dp + \frac{1}{2\Delta_i} \frac{F(\vec{p}_i^{(+)})}{G_f(p_i^{(+)})} \times \left[ \ln \left| \frac{(a_2 - p_i^{(-)})}{(a_2 - p_i^{(+)})} \frac{(a_1 - p_i^{(+)})}{(a_1 - p_i^{(-)})} \right| - i\pi \right], \quad (\text{C8a})$$

$$H_{p_i^{(-)}} = \int_{b_1}^{b_2} \frac{1}{G_i(\vec{p})} \left[ \frac{F(\vec{p})}{G_f(\vec{p})} - \frac{F(\vec{p}_i^{(-)})}{G_f(\vec{p}_i^{(-)})} \right] dp + \frac{1}{2\Delta_i} \frac{F(\vec{p}_i^{(-)})}{G_f(p_i^{(-)})} \times \left[ \ln \left| \frac{(b_2 - p_i^{(-)})}{(b_2 - p_i^{(+)})} \frac{(b_1 - p_i^{(+)})}{(b_1 - p_i^{(-)})} \right| - i\pi \right], \quad (\text{C8b})$$

$$H_{p_f^{(+)}} = \int_{c_1}^{c_2} \frac{1}{G_f(\vec{p})} \left[ \frac{F(\vec{p})}{G_i(\vec{p})} - \frac{F(\vec{p}_f^{(+)})}{G_i(\vec{p}_f^{(+)})} \right] dp + \frac{1}{2\Delta_f} \frac{F(\vec{p}_f^{(+)})}{G_i(p_f^{(+)})} \times \left[ \ln \left| \frac{(c_2 - p_f^{(-)})}{(c_2 - p_f^{(+)})} \frac{(c_1 - p_f^{(+)})}{(c_1 - p_f^{(-)})} \right| - i\pi \right], \quad (\text{C8c})$$

$$H_{p_f^{(-)}} = \int_{d_1}^{d_2} \frac{1}{G_f(\vec{p})} \left[ \frac{F(\vec{p})}{G_i(\vec{p})} - \frac{F(\vec{p}_f^{(-)})}{G_i(\vec{p}_f^{(-)})} \right] dp + \frac{1}{2\Delta_f} \frac{F(\vec{p}_f^{(-)})}{G_i(p_f^{(-)})} \times \left[ \ln \left| \frac{(d_2 - p_f^{(-)})}{(d_2 - p_f^{(+)})} \frac{(d_1 - p_f^{(+)})}{(d_1 - p_f^{(-)})} \right| - i\pi \right] \quad (\text{C8d})$$

where the domains  $[a_1:a_2] + [b_1:b_2] + [c_1:c_2] + [d_1:d_2]$  span  $[0:\infty]$  and contain the poles  $p_i^{(+)}$ ,  $p_i^{(-)}$ ,  $p_f^{(+)}$ , and  $p_f^{(-)}$ , respectively. In the event that  $p_\alpha^{(\pm)}$  does not exist in  $[0:\infty]$ , then our expressions require  $F(p_\alpha^{(\pm)}) = 0$ .

[1] J. A. Eden and M. F. Gari, Phys. Lett. B **347**, 187 (1995).  
[2] V. Herrmann, K. Nakayama, O. Scholten, and H. Arellano, Nucl. Phys. A **582**, 568 (1995).  
[3] M. Gari and H. Hyuga, Z. Phys A **277**, 291, (1976); Nucl. Phys. A **278**, 372 (1977).  
[4] F. E. Low, Phys. Rev. **110**, 974 (1958).  
[5] S. L. Adler and Y. Dothan, Phys. Rev. **151**, 1267 (1966).

[6] E. M. Nyman, Phys. Rev. **170**, 1628 (1968); Phys. Lett. **25B**, 135 (1967).  
[7] G. Felsner, Phys. Lett. **25B**, 290 (1967).  
[8] R. L. Workman and H. W. Fearing, Phys. Rev. C **34**, 780 (1986).  
[9] V. R. Brown, P. L. Anthony, and J. Franklin, Phys. Rev. C **44**, 1296 (1991).

- [10] V. Herrmann, J. Speth, and K. Nakayama, *Phys. Rev. C* **43**, 394 (1991).
- [11] V. Herrmann and K. Nakayama, *Phys. Rev. C* **46**, 2199 (1992).
- [12] H. W. Fearing, TRIUMF Report No. TRI-PP-93-12, (1993).
- [13] H. W. Fearing, Kernfysisch Versneller Instituut Report No. KVI-180i, 1992 (unpublished).
- [14] J. A. Eden, D. Plümper, M. F. Gari, and H. Hebach, *Z. Phys. A* **347** 145 (1993).
- [15] J. A. Eden and M. F. Gari, Ruhr Universität Bochum Report No. RUB-MEP-81/94; nucl-th/9501034.
- [16] A. Katsogiannis and K. Amos, *Phys. Rev. C* **47**, 1376 (1993).
- [17] M. Jetter, H. Freitag, and H. von Geramb, *Phys. Scr.* **48**, 229 (1993).
- [18] M. Jetter and H.V. von Geramb, *Phys. Rev. C* **49**, 1832 (1994).
- [19] M. Jetter and H. Fearing, TRIUMF Report No. TRI-pp-94-90; nucl-th/9410040.
- [20] F. de Jong, K. Nakayama, V. Herrmann, and O. Scholten, *Phys. Lett B* **333**, 1 (1994); F. de Jong, K. Nakayama, and T.-S. H. Lee, nucl-th/9412013.
- [21] V. R. Brown, *Phys. Rev.* **177**, 1498 (1969).
- [22] V. R. Brown, *Phys. Lett. B* **23**, 259 (1971).
- [23] J. Flender and M. F. Gari, *Phys. Rev. C* **51**, R1 (1995); *Z. Phys. A* **343**, 467 (1992).
- [24] T. D. Cohen, *Phys. Rec. D* **34**, 2187 (1986); N. Kaiser, U. G. Meissner, and W. Weise, *Phys. Lett. B* **198**, 75 (1988).
- [25] P. Alberto, E. Ruiz Arriola, M. Fiolhais, F. Grümmer, J. N. Urbano, and K. Goeke, *Phys. Lett. B* **208**, 75 (1988).
- [26] B. L. G. Bakker, B. Brozoian, J. N. Maslow and H. J. Weber, *Phys. Rev. C* **25**, 1134 (1982).
- [27] M. F. Gari and W. Krümpelmann, *Phys. Rev. D* **45**, 1817 (1992).
- [28] D. Plümper, J. Flender, and M. F. Gari, *Phys. Rev. C* **49**, 2370 (1994).
- [29] D. Huber, H. Witala, H. Kamada, and W. Glöckle, "Proceedings of the XVth European Conference on Few-Body Problems in Physics," FBXV Peñiscola, Spain (1995).
- [30] A. W. Thomas and K. Holinde, *Phys. Rev. Lett* **63**, 2025 (1989).
- [31] M. Gari, H. Hyuga, and B. Sommer, *Phys. Rev. C* **14**, 2169, (1976).
- [32] G.-H. Niephaus, M. Gari, and B. Sommer, *Phys. Rev. C* **20**, 1096, (1979).
- [33] M. Gari, G.-H. Niephaus, and B. Sommer, *Phys. Rev. C* **23**, 504, (1981).
- [34] W. N. Cottingham, M. Lacombe, B. Loiseau, J. M. Richard, and R. Vinh Mau, *Phys. Rev. D* **8**, 800 (1973); M. Lacombe, B. Loiseau, J. M. Richard, R. Vinh Mau, J. Côté, P. Pirés, and R. de Tourreil, *Phys. Rev. C* **21**, 861 (1980).
- [35] K. Michaelian *et al.*, *Phys. Rev. C* **41**, 2689 (1990). **21**, 861 (1980).
- [36] D. Drechsel and L. V. Maximon, *Ann. Phys. (NY)* **49**, 403 (1968).
- [37] D. O. Riska, "Exchange currents," University of Helsinki Report No. HU-TFT-89-15.
- [38] M. Araki and N. Kamal, *Phys. Rev. D* **29**, 1345 (1984).
- [39] C. D. de Tar, *Phys. Rev. D* **24**, 752 (1981); *D* **24**, 762 (1981).
- [40] S. Deister, M. F. Gari, W. Krümpelmann, and M. Mahlke, *Few Body Syst.* **10**, 1 (1991).
- [41] U. Karlsruh and M. F. Gari, *Nucl Phys* **A408**, 507 (1983).
- [42] M. Chemtob, E. Moniz, and M. Rho, *Phys. Rev. C* **10**, 344 (1974).
- [43] E. Hummel and J. A. Tjon, *Phys. Rev. Lett.* **63**, 1788 (1989).
- [44] Particle Data Group, *Rev. Mod. Phys.* **52**, 2II, 81 (1980); O. Dumbrajs, R. Koch, H. Pilkuhn, G. C. Oades, H. Behrens, J. J. de Swart, and P. Knoll, *Nucl. Phys.* **B216**, 277 (1983).
- [45] G. E. Brown and W. Weise, *Phys. Rep. C* **22**, 279 (1975).
- [46] A. M. Green *et al.*, *Rep. Prog. Phys.* **39**, 1109 (1976).
- [47] T. Ericson and W. Weise, *Pions and Nuclei* (Clarendon Press, Oxford, 1988).
- [48] H. Arenhövel, *Nucl. Phys.* **A247**, 473 (1975).
- [49] R. Machleidt, K. Holinde, and C. Elster, *Phys. Rep.* **149**, 1 (1987); R. Machleidt, *Adv. Nucl. Phys* **19**, 189 (1989).
- [50] L. L. Foldy, *Phys. Rev.* **122**, 275 (1961).
- [51] R. A. Krafcik and L. L. Foldy, *Phys. Rev. Lett.* **24**, 545 (1970); *Phys. Rev. D* **10**, 1777 (1974).
- [52] J. L. Friar, *Phys. Rev. C* **12**, 695 (1975). *Phys. Rev. D* **10**, 1777 (1974).
- [53] W. Glöckle and L. Müller, *Phys. Rev. C* **23**, 1183 (1980).
- [54] M. M. Nagels, T. A. Rijken, and J. J. de Swart, *Phys. Rev. D* **17**, 768 (1978).
- [55] S. Weinberg, *Phys. Rev. Lett.* **18**, 188 (1967).
- [56] J. Wess and B. Zumino, *Phys. Rev.* **163**, 1727 (1967).
- [57] F. Gross, *Phys. Rev. C* **26**, 2203 (1982).
- [58] F. Gross, K. M. Maung, J. A. Tjon, L. W. Townsend, and S. J. Wallace, *Phys. Rev. C* **40**, R10 (1989).
- [59] F. Gross, J. W. Van Orden, and K. Holinde, *Phys. Rev. C* **41**, R1909 (1990).
- [60] R. M. Woloshyn and A. D. Jackson, *Nucl. Phys. B* **64**, 269 (1973).
- [61] J. Fleischer and J. A. Tjon, *Nucl. Phys. B* **84**, 375 (1975).
- [62] E. Erkelenz, *Phys. Rep. C* **13**, 193 (1974).